SUM4Re

Creating materials banks
from digital urban mining

D10.3: Strategic planning and data collection report 3

VERSION 1.0

30 October 2025

PUBLIC

Associated with document Ref. 101129961

Funded by the European Union. Views and opinions expressed are however those of the author(s) only and do not necessarily reflect those of the European Union. Neither the European Union nor the granting authority can be held responsible for them.

Funded by the European Union

SUM4Re

Creating materials banks from digital urban mining

Deliverable ID	10.3
Deliverable name	Strategic planning and data collection report 3
Lead partner	SINTEF
Contributors	AFDECOM, NORSKE, UVIGO, VTT, EAGLE, BLOCK MATERIALS, CONCULAR

Funded by the European Union

DOCUMENT INFORMATION

Document name	D10.3 Strategic planning and data collection report 3
Version	1.0
Due date	2025.10.31
Report date	2025.10.30
Number of pages	67
Lead Author	Sveinung Nesheim (SINTEF)
Other Authors	Ramon Hingorani (SINTEF), Emil Kristoffer Lindberg (NORSKE), Jesús Balado-Frías (UVIGO), Ourania Patsia (EAGLE), Francisco Senna Vieira (VTT), Tom Lacroix (BLOCK), Benjamin Lammers (CONCULAR),
Dissemination level	Public

REVISION HISTORY

Rev.	Date	Description of revision
0.1	26/09/2025	Submitted for review
0.2	24/10/2025	Revised version
1.0	30/10/2025	Final version

DOCUMENT APPROVAL

Written	Sveinung Ørjan Nesheim (SINTEF)	26/09/2025
Revised	Helen van Broekhuijsen (THUAS), Ger Kwakkel (CTH)	24/10/2025
	Ana Sánchez Rodríguez (UVIGO, Project Manager)	30/10/2025
Approved	Pedro Arias Sánchez (UVIGO, Project Coordinator)	30/10/2025

EXECUTIVE SUMMARY

As part of Work Area 6: Demonstrators in Existing Built Works, Task 10.3 in Work Package 10 has focused on establishing a baseline assessment for the Svalbard pilot site in Longyearbyen. The objective has been to develop a strategic plan for pilot implementation and testing, supported by the identification, analysis, and digitalization of the pilot building. This preparatory work provides the technical basis for subsequent pilot activities in Work Package 11 where analysis of the harvested data will be conducted.

Field activities were carried out in two phases during spring 2025. On 28–29 May, VTT conducted an external scan of the pilot building using Active Hyperspectral Sensing (AHS). The purpose of this activity was to record information on the condition and quality of timber cladding of the building envelope. On 13–14 June, additional scanning was conducted. Here the University of Vigo (UVIGO) applied an Augmented Reality Mobile Mapping System (AR iMMS-RGB) combined with LiDAR through an integrated HoloLens device to capture spatial and visual data, while EAGLE carried out Ground Penetrating Radar (GPR) scanning of both external and internal areas to map structural layers and subsurface conditions. All scanning activities proceeded according to plan. Each building has its own particulars and conditions and it is difficult to generalize about what to expect from planning, but in the case of the Svalbard pilot these condition was favourable and the scanning was executed without particular issues or delays.

In parallel with the scanning, a manual materials inventory was completed. The results are populated in CIRDAX and CONCULAR databases, following the agreed formats for data entry. Information about the required labour input has also been recorded to support later evaluations.

The baseline assessment also incorporates a review of legal, functional, and environmental aspects relevant for the reuse of materials and the implementation of the pilot. This includes (i) legal requirements such as general legislation, rules and standards for reuse, and potential regulatory barriers or opportunities; (ii) functional considerations related to structural integrity, thermal performance, moisture behaviour, adaptability of the building, and expected remaining service life; and (iii) environmental aspects, including the influence of the Arctic climate on energy needs, comparisons between new construction and reuse strategies, risks of contaminated components, and the need for holistic assessments.

The combined outcomes of the scanning campaigns, the manual materials inventory, and the review of contextual aspects form a baseline dataset for the Svalbard pilot. This includes information on the condition of the building structure, material quantities, spatial configuration, and the framework conditions for reuse. The dataset will be used as input for the continuous development of a material database in the next steps of the pilot implementation, where identification of the highest circular value of CDW in relation to local business opportunities and requirements will be pursued.

GLOSSARY

Terms, Abbreviations, and Acronyms

HBIM	Historic Building Information Modelling
AR iMMS-RGB	Augmented Reality integrated Mobile Mapping System
AHS	Active Hyperspectral Sensing
GPR	Ground penetrating radar
HaDEA	European Health and Digital Executive Agency
CDW	Construction and Demolition Waste
LiDAR	Light detection and ranging/Laser imaging, detection, and ranging is a method for determining ranges by targeting an object or a surface with a laser and measuring the time for the reflected light to return to the receiver.
NDT	Non-Destructive Testing
EM	Electromagnetic
ML	Machine Learning
NIR	Near-infrared
HSI	Hyperspectral imaging
SC	Supercontinuum (in context of laser technology)
DMS	Dielectric moisture sensing
IRT	Infrared thermography
RGB	Red Green Blue in context of colour models
ToF	Time of Flight in context of Lidar technology
HMLS	Handheld Mobile Laser Scanner
IMU	Inertial measurement unit
MEMS-FPI	Microelectromechanical Fabry-Perot interferometer
FWHM	Full width at half maximum
SFCW	Step-frequency continuous-wave

TABLE OF CONTENTS

LIST OF TABLES

LIST OF FIGURES

1. Introduction

1.1. About SUM4re

The SUM4Re (Creating Material Banks from Digital Urban Mining) project is a research initiative under the Horizon Europe Programme, targeting intelligent data acquisition and analysis of materials and products in existing built environments. The project aims to facilitate urban mining—the systematic identification, extraction, and reuse of construction materials—to enhance circularity and reduce waste in the construction sector. SUM4Re will be validated through 15 Use Cases (UCs) addressing different challenges in material identification, data integration, and market adoption. The project will conduct three large-scale pilot studies in Norway, the Netherlands, and Spain, each targeting different building types and material categories. SUM4Re aligns with the EU Green Deal and Circular Economy Action Plan, aiming to create scalable solutions for sustainable construction and material reuse.

1.2. Objectives of WP10

WP10 is an assessment of the baseline and the strategic planning for the implementation and testing activities of the Svalbard pilot site. This deliverable provides detailed methodologies for data acquisition, material inventory generation, and strategic scheduling to ensure the successful application of circular construction principles.

Objectives:

- Assess the baseline conditions of the Svalbard pilot site.
- Develop a strategic plan for pilot implementation and testing activities.
- Establish protocols for identifying, analyzing, and digitalizing demonstrators.
- Create a comprehensive material inventory registered in digital material databases (CIRDAX and CONCULAR).

1.3. About the Svalbard pilot

The Svalbard pilot stands out as one of the most challenging and innovative aspects of the SUM4Re project due to its extreme environmental conditions, logistical constraints, and urgent need for circular solutions. It focuses on the reuse and renovation of residential buildings in Longyearbyen, a town facing severe structural issues due to thawing permafrost. The buildings in Longyearbyen are sinking, shifting, and developing structural issues, leading to increased maintenance costs and safety risks. Remote Arctic locations like Svalbard have limited access to new construction materials, making reuse and recycling crucial for sustainable development.

The pilot building (Figure 1) was originally constructed in 2005 as a modular residential building. Its prefabricated modules were transported to Longyearbyen and assembled rapidly, reflecting a construction strategy well aligned with Svalbard's short building season and logistical constraints.

Key advantages of the modular approach included[1]:

- production carried out indoors, avoiding critical construction activities in snow and rain
- fast delivery, since foundation work and factory production could proceed in parallel
- possibility to relocate the building if future needs changed
- reduced responsibility and construction risk for the client due to controlled off-site production
- excellent thermal performance, particularly regarding airtightness and insulation

[1] Hålogaland Element AS (2005). Project: Elvesletta Nord, Longyearbyen – Residential Housing. *Description Version 1.2*

Figure 1. Pilot building in Svalbard (left: front side; right: rear side)

At the outset of SUM4Re, building module relocation was intended: the building modules were foreseen to be disassembled and reassembled at a different site in Svalbard, demonstrating direct reuse of whole modules. Although this plan was later withdrawn due to economic and other practical reasons, the concept remains highly relevant since many similar buildings may face the same destiny as ground conditions continue to evolve.

Therefore, investigating the feasibility of both full-module reuse and selective reuse of high-value components (e.g., windows, doors, structural timber) is essential to unlock circular value in Svalbard's housing stock. This pilot serves as a demonstrator for scalable Arctic-proof circular construction solutions benefiting communities with constrained material access worldwide.

1.4. About deliverable D10.3

D10.3 (Strategic Planning and Data Collection Report) is the deliverable of task T10.3. T10.3 is dedicated to preparing the baseline assessment pilot site, covering legal, functional, environmental, and economic factors that influence circular construction in Svalbard (section 2). Section 3 presents the innovative scanning technologies used at the pilot site to collect data on the building, its components and materials. This is followed by section 4, which summarizes the on-site data acquisition planning. Finally, section 5 describes the implementation of the data acquisition campaign and a description of the results obtained. The analysis and interpretation of these results will be the objective of WP11, which will also address the assessment of the corresponding KPIs, aiming at demonstrating a 50 % reduction in time for geometry and material data acquisition and up to a 90 % productivity increase compared to traditional manual inventories (Project KPI7)

D10.3 has been led by SINTEF in collaboration with Store Norske Boliger, AF Decom, Block Materials, University of Vigo, VTT, and Screening Eagle.

2. Baseline assessment

This section addresses the foundational aspects required for understanding the unique conditions of the Svalbard site. The assessment summarizes legal, functional, environmental, and economic factors that influence the execution of circular construction principles in an Arctic context.

2.1. Legal aspects

A summarizing overview of the key legal requirements and standards that regulate the reuse of building materials on Svalbard is given below. This encompasses both general provisions

in national legislation and specific conditions that apply to Svalbard. A more detailed description of this topic is given in Deliverable D.1.2.

2.1.1. General Legislation and Regulations

- **Planning and Building Act (PBA):** On Svalbard, the same legislation as on the mainland generally applies, but with certain regulatory adaptations and differences in practice. Reuse must adhere to documentation requirements regarding load-bearing capacity, fire protection, and suitability for use.
- **Building Regulations (TEK):** Establishes minimum requirements for construction, fire safety, energy efficiency, and indoor climate. When reusing components, it is crucial to ensure these requirements remain fulfilled.
- **Svalbard Treaty and Local Provisions:** Svalbard has specific rules through local governance (Longyearbyen Community Council) that can influence permitting and administrative processes.

2.1.2. Rules and Standards for Reuse

- **CE Marking and Product Documentation:** Used materials may lack valid documentation, which can create the need for new or supplementary evidence of compliance.
- **National Standards/NS-EN:** Building parts are often required to still meet relevant standards—for instance, Eurocodes for load-bearing structures or standards for fire classification and insulation.
- **Experience from SirkTRE:** Demonstrates that clear documentation of quality, remaining service life, and suitability for the intended use is crucial for authorities to approve reused materials.

2.1.3. Legal Barriers and Opportunities

- **Requirement for Documented Safety:** When reusing components, authorities may demand closer scrutiny and verification compared to standard new purchases.
- **Svalbard's Land-Use Plan and Building Boundaries:** Renovations or reuse may be subject to stricter application and permitting processes due to environmental considerations.
- **Potential for Streamlining:** New guidelines and pilot projects can help simplify reuse in the future if documentation requirements become more standardized.

2.1.4. Summary

- **General:** Legislation on Svalbard largely aligns with mainland Norway, but features unique administrative processes and practical implications.
- **Reuse:** Often requires more documentation and quality assurance than using new components.
- **Further Steps:** It is advisable to investigate specific local rules under the Longyearbyen Community Council, as well as potential exemptions for reusing older building elements. A thorough plan for legal documentation and compliance with relevant standards will ensure a lawful and robust outcome.

2.2. Functional aspects

The functional performance of buildings on Svalbard is strongly influenced by a combination of Arctic climate and permafrost. Cold temperatures and high winds demand, among other things, high insulation levels and robust construction to ensure indoor climate comfort,

structural stability, and long service life. When assessing the reuse of existing components, the following considerations should be part of the baseline analysis:

2.2.1. Structural Integrity:

Older load-bearing elements must demonstrate sufficient capacity to meet modern standards for wind and snow loads. Wear, moisture damage, and corrosion can be critical factors, especially when permafrost undergoes repeated freezing and thawing processes.

2.2.2. Thermal Properties:

Due to higher energy demands on Svalbard compared to the mainland, components like windows, exterior walls, and roofs with inadequate insulation values can result in elevated operating costs. Therefore, evaluating U-values and airtightness is essential.

2.2.3. Moisture and Condensation:

Despite cold and relatively dry conditions, temperature fluctuations and potential moisture intrusion can lead to condensation problems. Thus, reuse should only proceed after a thorough condition assessment that identifies any moisture-related damage.

2.2.4. Adaptability:

Older building elements are often designed to meet different standards and purposes. When reusing an element, it is crucial to determine whether it is suitable for the new function (floor plan, fire safety, room height requirements, etc.).

2.2.5. Remaining Service Life:

If a component is nearing the end of its operational lifespan, investing in the necessary adaptations and refurbishment may be less advisable. An accurate technical assessment is therefore essential to avoid unnecessary costs and redesign in the future.

2.2.6. Summary

Successful reuse on Svalbard requires that load-bearing, thermal, and moisture-related properties remain adequate under Arctic conditions. By balancing remaining service life, upgrade needs, and potential reuse benefits, one can determine whether reuse is a sensible solution—both technically and economically.

2.3. Environmental aspects

Svalbard has a unique ecosystem characterized by permafrost and sparse vegetation, where even minor disturbances can have long-term consequences for wildlife and plant life. The land-use plan for Longyearbyen stipulates that the city's footprint must not exceed defined boundaries, thereby preserving the untouched nature of the surrounding areas. Nevertheless, certain interventions are permitted within the plan area, even if they may affect local wildlife.

2.3.1. Extreme climate and energy needs:

Low temperatures and frequent, intense winds on Svalbard increase the demand for highly efficient building envelopes with effective insulation and airtightness. Older buildings can be less energy-efficient, resulting in higher heat loss and thus greater reliance on fossil fuel (diesel) during operation.

2.3.2. New construction vs. reuse:

Although reuse reduces the transportation of new materials, a building with substantially higher energy consumption over its lifetime may produce larger overall emissions than a newly constructed building featuring modern, energy-saving designs. In some cases, it may therefore be more environmentally advantageous in the long run to demolish and rebuild, rather than to reuse a building shell that is highly inefficient to operate. It can be noticed that buildings erected in Longyearbyen around 2005 were modular systems shipped from mainland Norway, designed for rapid installation and moderate durability for arctic conditions.

At that time, Longyearbyen was transitioning from a temporary mining town to a civilian community, and these buildings were considered semi-permanent. Their expected service life was typically 20–30 years. Currently, buildings in Longyearbyen are designed as permanent, climate-resilient structures with an expected service life of 50 years or more, using steel foundations to bedrock, improved insulation, and construction methods adapted to thawing permafrost.

2.3.3. Contaminated components:

Before any demolition, an environmental survey is generally conducted to identify hazardous substances such as asbestos, heavy metals, or PCBs. All waste must be sorted and transported to approved disposal facilities on the mainland, as Svalbard does not have its own local waste processing plant for this kind.

2.3.4. Holistic assessment:

All materials used on Svalbard are shipped in, contributing to an additional transport footprint. At the same time, power generation is off-grid and predominantly reliant on fossil fuels. When comparing reuse and new construction, one must weigh the short-term benefits of reuse (reduced waste and reduced import of new materials) against the long-term gains of a more energy-efficient new structure in a challenging Arctic environment.

2.3.5. Summary

Svalbard's fragile Arctic ecosystem demands careful balancing of development and preservation. Longyearbyen's land-use plan limits expansion, but interventions within city boundaries still affect nature. The extreme climate drives high energy needs, making efficient building envelopes essential; older buildings often depend heavily on fossil fuels. While reuse reduces waste and transport, inefficient structures may cause higher lifetime emissions than new, energy-optimized buildings. Hazardous components must be identified and shipped to the mainland for safe disposal. Overall, decisions on reuse versus new construction require a holistic view that weighs short-term material savings against long-term environmental performance in challenging Arctic conditions.

2.4. Economic aspects

On Svalbard, the economic conditions differ markedly from those on the mainland. Labor is more expensive, partly due to high housing costs and a small service market, and the transportation of materials to the archipelago also entails added expenses. In addition, energy prices are high, which often makes it more profitable to invest in modern, energy-efficient building components than to reuse older ones with poor insulation performance.

For example, reusing doors or windows with weak U-values can lead to greater heat loss and, thus, higher operating costs over time. At the same time, dismantling and upgrading such elements is labor-intensive, further increasing project expenses. If a reused component has limited remaining service life, the total cost may be high compared with purchasing new components.

In summary, these special circumstances—costly labor, expensive logistics, and relatively high energy prices—should be factored into a comprehensive assessment of whether reuse is truly economically advantageous on Svalbard. The combination of high costs and a carbon-intensive energy supply means that labor-intensive dismantling and refurbishment work can quickly become both expensive and emissions-heavy. As a result, reuse strategies tend to focus on components that are easy to handle, standardised, and adaptable for local reuse, while more complex recovery or refurbishment processes are often avoided.

2.5. Link between building context, circularity challenges and data acquisition needs

The baseline assessment has shown that the potential for circular use of the pilot building's components is strongly influenced by its Arctic context. Legal documentation requirements (section 2.1), functional requirements, such as e.g. high insulation and moisture-protection need (section 2.2), environmental effects of primarily fossil-based operation (section 2.3), and the elevated cost of labour and logistics in Svalbard (section 2.4) all increase the threshold for economically viable reuse.

Initially, the pilot modules were intended to be disassembled and relocated to a new site within Longyearbyen (section 1.3). This intention underlined the possibility for direct reuse of whole modules, which represents the highest circular value pathway for this building type, as most embedded environmental impact and technical function is preserved. Even though the relocation plan was later withdrawn, the assessment of module-level reuse remains a key ambition of this pilot and directly informs the data acquisition strategy. In addition, component-level reuse is an important option.

The building is composed predominantly of timber-based modular structures, where circular value depends strongly on the actual state of hidden layers and fastening systems. As summarised in Table 1, some elements (e.g., gypsum boards, particle boards) exhibit low reuse potential due to dismantling damage, while others (e.g., windows, doors, structural timber elements) have high reuse value but require clear documentation of integrity and performance. For certain components—insulation layers, structural studs, moisture-exposed cladding—the decision between upgrading in place, selective reuse, or downcycling depends on detailed condition information that is not available from design drawings alone.

These aspects define the core information needs addressed by the data acquisition campaign:

- AR iMMS-RGB mapping supports complete digital traceability of both entire building modules and components, enabling safe disassembly planning and verification of dimensional stability for potential relocation or integration elsewhere.
- AHS scanning focuses on the external cladding and other surfaces subject to harsh weathering, providing insight into degradation, coatings, and moisture effects, necessary for condition and durability assessment.
- GPR identifies hidden characteristics of timber assemblies concealed studs, joints, potential voids and insulation continuity, enabling non-destructive evaluation of elements critical to reuse and dismantlability.
- Thermography and dielectric moisture sensing supply boundary-condition measurements for understanding the building's exposure conditions.

The data collected by these technologies (section 3-5) bridges the gap between contextual constraints and circular opportunities. It ensures that subsequent analyses focus on the components and assemblies with the greatest influence on circular value creation in Svalbard, supporting strategic decisions on selective dismantling, reuse of components, potential module relocation, and necessary upgrade measures.

Table 1. Key constructions products of the Svalbard pilot and their potential circularity strategies

Products	Circularity strategy
1) Structural timber and Glulam (Glued laminated timber)	The timber in the modules are all of small dimensions and volumes. The dismantling is cumbersome due to the amount of fasteners. Damages from dismantling expected. Circularity as chips or small standardized lengths most probable.
2) Chipboard (Particle board)	Cumbersome dismantling with high degree of damages. In practice low potential of salvaging.
3) Exterior and interior wood cladding	Exterior cladding easy to dismantle, but short lengths lower the reusability potential. Interior cladding with low circularity potential due to short lengths and damages. Reuse as chips.
4) Parquet and laminate flooring	Flooring with some potential for salvaging and reuse. Easy to dismantle without damages.
5) Mineral wool (insulation based on stone or glass)	Insulation may be reused unless damp, but the required labour cost is high compared to cost of new product. New product is light and require little energy to transport.
6) Plastic (vapor barrier)	No reusability potential as film. Recycle.
7) Gypsum boards (Drywall)	Difficult to dismantle without severe damage. Little potential for reuse, however it is a heavy product with high embodied energy.
8) Wood fiberboard (Soft and Hard/MDF)	Depending on the original use challenges to dismantle without damage. Probably downcycled and conveyed as chips.
9) Steel (Rebars, profiles and brackets)	H- and I-beams with huge potential of direct reuse. Else less potential other than recycling.
10) Concrete (slabs, screed, and columns/beams)	There are no slabs as decks or walls in the pilot, but minor slabs may be found. The potential for reuse of these are low. Crushing and reuse as fill may be an option if the toxic control is sufficient.
11) Windows	Windows high reusability as original product in Svalbard and in the arctic. Marked price much higher than the mainland, and cost and eCO2 associated with transport is high. Challenges with increased energy use in buildings with old windows due to polluting energy mix on Svalbard.
12) Doors	As for windows.
13) Complete modules	Reusing the whole modules is by far the most promising type of reuse on Svalbard and the arctics due to the associated conservation of embedded eCO2 from manufacturing and transport of the module from mainland. The module may require repair (moisture barrier and deformations), but this may be a done locally in combination with increased insulation (internally or externally).

2.6. Manual material inventory

The material inventory focuses on categorizing components and registering them in digital databases to facilitate traceability and circular workflows. Data will be integrated into CIRDAX and CONCULAR using standardized protocols, enabling interoperability and lifecycle tracking. This process is guided by the principles of a Pre-Demolition Audit (PDA) according to DIN SPEC 91484, with the aim of assessing the potential for high-quality reutilization.

2.6.1. Key Data Parameters for CIRDAX and CONCULAR

Given the intention of UVigo to extract data into the databases in an automated manner, a clear definition of the required parameters is essential. The following information is considered critical for a meaningful assessment and successful data integration:

- Condition of the materials: A detailed visual assessment of the current physical state, noting any damage, wear, tear, or discoloration that could affect its potential for reuse.
- History of the material (Refurbished/Replaced): An investigation into the component's history to determine if it has been previously refurbished or if it replaced an original element. This provides insight into its lifecycle and durability.
- Connection and Fastening Methods: A precise analysis of how the different components are fastened to each other (e.g., screwed, glued, welded, clipped). This is critical for assessing the dismantlability and the potential for non-destructive removal.

2.6.2. Inventory of materials

Using the archival drawings obtained from the pilot project, a comprehensive desk study was conducted. The drawings and documents provided substantial insight into the structural composition and spatial layout of the building, allowing for the preliminary identification and quantification of numerous construction and layout elements. Dividing the project into two units (top and bottom), the definition of units was specified.

Inspection on-site was not foreseen in this task, given the pilot's location on Svalbard and the associated travel costs and climate burden. The drawings and documents were reviewed and determined to provide sufficiently good insight for the project (with the exception of information on the condition of the building components, which requires actual inspection). The missing information from the potential site visit was therefore deemed unlikely to adversely affect the further development of the project. Finally, the detailed desk study and subsequent data entry into the Cirdax system has been completed and shared with SINTEF and Concular.

2.6.3. Registration of data in CIRDAX and CONCULAR

Workflow and data collection

The workflow to complete the audit includes the following steps:

- **Data Analysis:** The data already collected from the Desk Study is further analyzed.
- **Planned Building Inspection:** In a standard process, a physical on-site inspection would normally be the next step to compare the data from the plans with the actual conditions. In this pilot, such an inspection was not carried out (see section 2.6.2).
- **Detailed Inventory:** If the inspection had been conducted, components would have been assessed on-site, and specific information important for the Cirdax and Concular databases would have been recorded, as required by the DIN SPEC for a detailed assessment:
    - **Condition of the materials** (e.g., damage, wear and tear).
    - Information on previous use (Was the material **refurbished** or **replaced**?).
    - **How the different components are fastened to each other** to assess dismantlability.

- **Data Processing:** After the optional inspection, the inventoried data would be processed and merged with the already existing information.
- **Error Correction:** Any errors or missing information would then be manually corrected.
- **Result Documentation:** The process culminates in the creation of the final documentation, which forms the basis for the reuse strategy. In line with the DIN SPEC, final reports will be generated from this, which can be referred to as a **Building Passport** and specific **Material Passports**.

Manual scan plan for the pilot buildings

Upon receiving a request to carry out a building inventory, the first step in our protocol involves gathering all available documentation related to the building. This may include architectural drawings, budgets, reports, specifications, and maintenance records. These documents serve as the foundation for an initial desk study, allowing us to form a preliminary understanding of the building's structure and material composition.

During this desk-based phase, we analyse the available data to identify the materials, layers, and structural systems within the building. This process also helps us pinpoint areas where on-site verification or additional field data could have been required. Based on this preliminary analysis, we formulate targeted questions and define data gaps that an inspection would normally address.

In a standard procedure, a site visit would then be scheduled in consultation with the building owner. If such a manual on-site inventory had been carried out, it would have allowed verification of the building's actual condition against the documentation, the collection of field measurements, scans, and photographs, as well as qualitative input from the owner regarding maintenance history and past renovations.

In this pilot, however, the manual on-site inventory was not conducted (see section 2.6.2) . Instead, the desk study and document-based analysis formed the complete basis for registration in Cirdax.

Within Cirdax, and with a similar process in Concular's software, materials and products identified from the desk study documents are manually and systematically categorised and documented in detail by inventory specialists. This manually entered data, based on the available documentation, is reviewed and enriched with photographs where necessary (e.g., from existing records if available). A second inventory specialist performs a quality check on this manually entered information, providing annotations or corrections where appropriate directly within the system.Once the complete dataset, derived from the desk study analysis, has been manually entered into the Cirdax system, it undergoes automated processing. The system scans the entered data for inconsistencies, missing information (based on expected fields), or potential errors. Any identified issues flagged by the system are then reviewed and corrected manually by the specialists to ensure the integrity and completeness of the dataset based on the source documents. Following this validation process, the system proceeds to perform advanced calculations related to cost estimation, CO_2 impact, and reuse potential based on the validated, manually entered data. Figure 2 provides an example screenshot showing uploaded building products within the CircularLCA system, which utilizes such data for analysis.

The output of this process is twofold:

1. A Building Passport, which consolidates all findings into a comprehensive document.
2. A set of Material Passports, which contain detailed, product-specific information.

In addition to these deliverables, the client receives access credentials to the Cirdax platform, along with an export of the complete dataset. This full package represents the final output of

the inventory process and serves as a critical resource for circular construction planning and material reuse strategies.

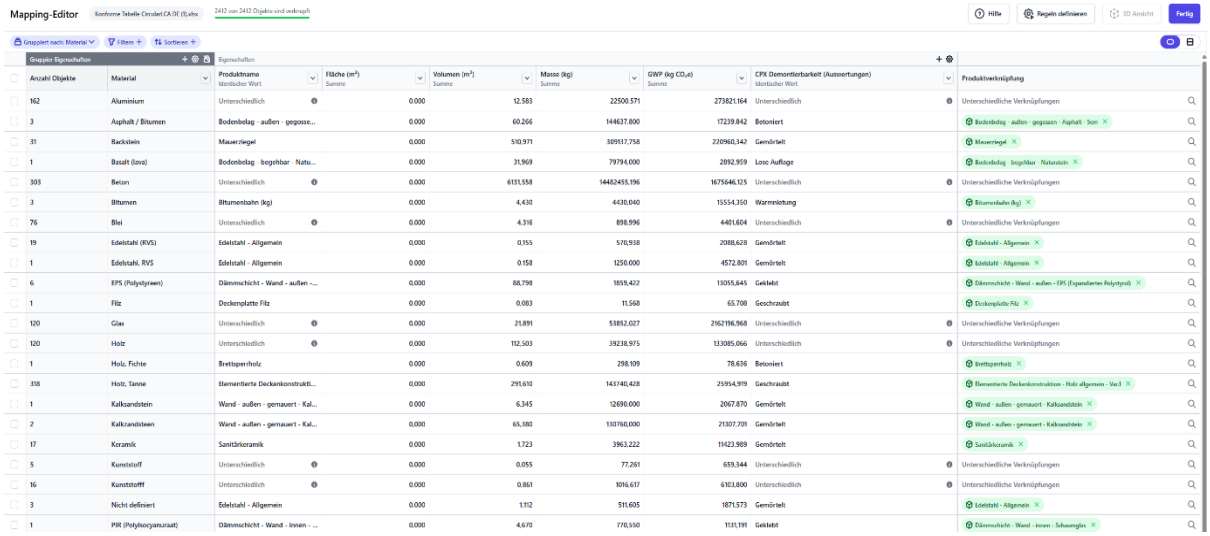

Figure 2. Screenshot of uploaded building products in CircularLCA. NL Pilot

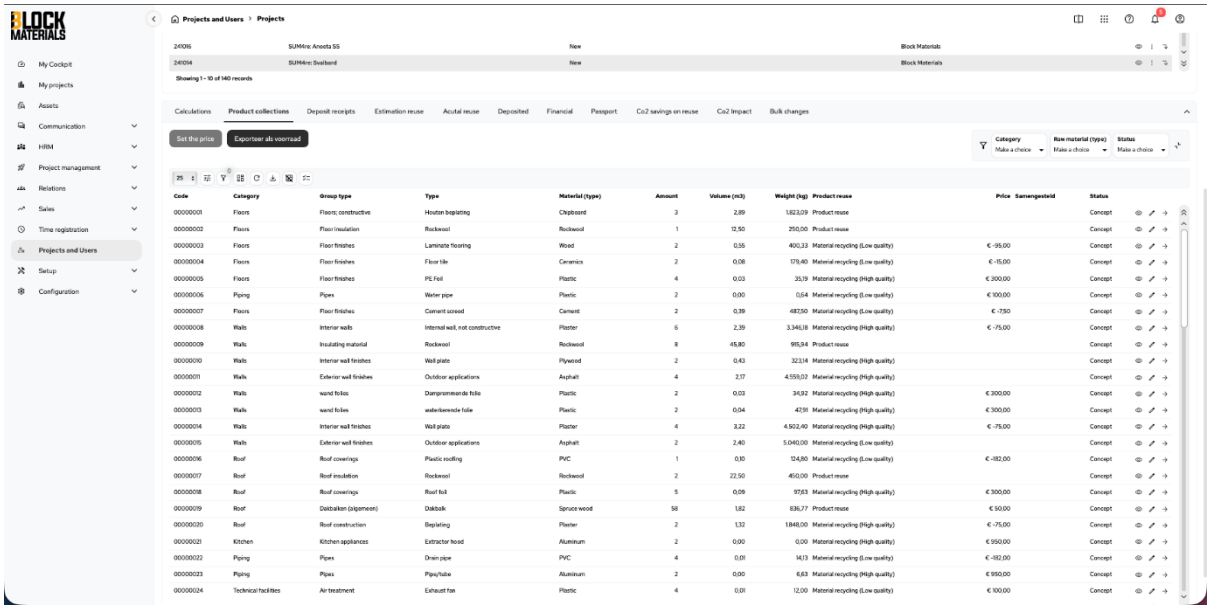

Figure 3. Screenshot of uploaded building products & materials in Cirdax. NO Pilot

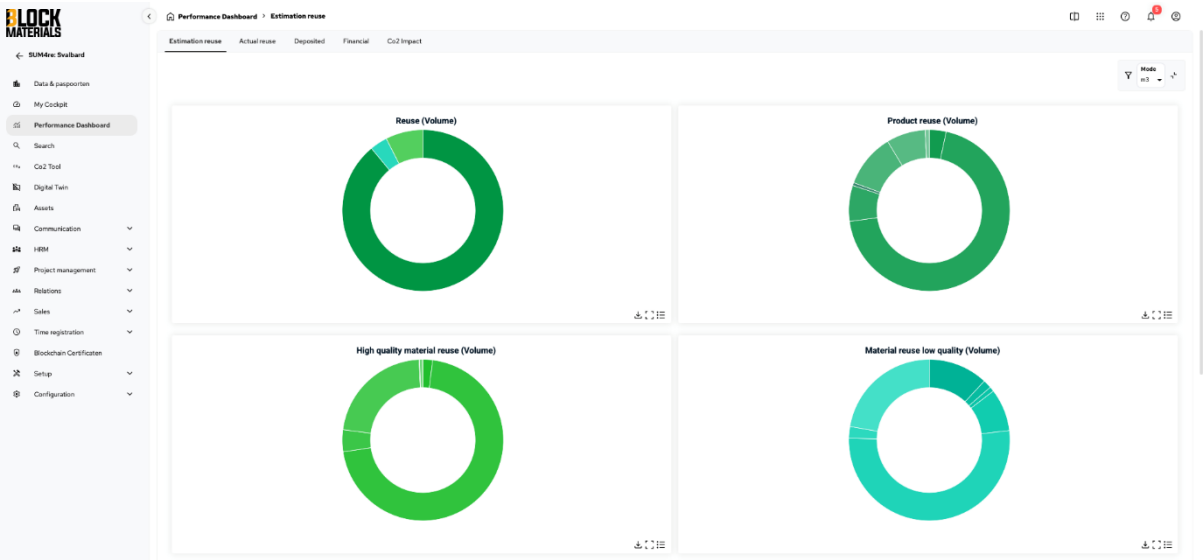

Figure 4. Screenshot of building performance dashboard in Cirdax. NO Pilot

2.6.4. Labour productivity

A fundamental parameter to assess the benefits of automated data acquisition and tracking in digital platforms for the sake of circular construction is the time. Table 2 summarizes the time needed for different subprocesses of the manual inventory, resulting in a total time of 37 hours.

Table 2. Time needed for the manual inventory

Resolution	Manual inventory
Collecting archive drawings	2 hours
Arranging Cirdax and sorting archive drawings	2 hours
Manual inventory Target Building	30 hours
Complete in Cirdax	3 hours
Total	37 hours (2 units)

3. Technical brief

The data collection at the Svalbard site includes three different scanning technologies:

- Augmented Reality integrated Mobile Mapping System (AR iMMS-RGB)
- Active Hyperspectral Sensing (AHS)
- Ground penetrating radar (GPR)

A brief SOA overview of building scanning technologies is given in section 3.1, followed by a more specific description of the equipment used in the Svalbard pilot in sections 3.2 and 3.3. Section 3.4 describes necessary preparatory measures performed. Finally, section 3.5 contains the sampling methods and procedures used in the data acquisition campaign.

3.1. State of the art of scanning technologies

3.1.1. LiDAR scanning

LiDAR technology has been successfully integrated with parametric modelling in Historic Building Information Modelling (HBIM) applications. Timber structures often exhibit complex geometries that challenge traditional surveying methods. Semi-automated methodologies developed in recent years for modelling timber trusses in historical buildings demonstrates the effectiveness of LiDAR for obtaining accurate structural representations to create 3D models in DXF format with standard deviation of 0.69%[2], distinguishing between the apparent cross-section and the resistant cross-section[3], detecting and analysing cracks (wider than 3 mm) in timber beams[4].

LiDAR-generated point clouds support advanced digital modelling techniques, including HBIM and finite element analysis (FEA), facilitating comprehensive structural evaluations. Portable LiDAR devices, such as smartphones and tablets, further enhance accessibility by allowing real-time damage detection and data sharing through cloud-based platforms[5].

Despite its benefits, LiDAR has certain limitations. The accuracy of LiDAR data is highly dependent on proper acquisition conditions, including optimal scanning angles and minimal occlusions. Gaps and occlusions in point clouds, caused by objects or people in the environment during acquisition, can lead to incomplete models, necessitating manual corrections. The presence of people, especially in large numbers or near the scanner, can significantly obstruct the laser beam, preventing the sensor from capturing parts of the surrounding surfaces. In such cases, reconstructing the missing parts of the point cloud often requires the operator to make assumptions about the geometry of non-visible or unscanned areas. These assumptions are typically based on prior knowledge of the scene, architectural regularities, or contextual information from adjacent structures, which allows for an informed approximation of the original shapes. While this process can restore the visual and geometric continuity of the model, it also introduces a degree of subjectivity and potential deviation from the actual physical environment[6].

To the best of the authors' knowledge, LiDAR applications in timber appear to be limited to the context of historic buildings and timber beams, and not to general building and other

[2] Otero, R., Lagüela, S., Cabaleiro, M., Sousa, H. S., & Arias, P. (2023, January). Semi-automatic 3D frame modelling of wooden trusses using indoor point clouds. In *Structures* (Vol. 47, pp. 1743-1753).

[3] Santos, D., Cabaleiro, M., Sousa, H. S., & Branco, J. M. (2022). Apparent and resistant section parametric modelling of timber structures in HBIM. *Journal of Building Engineering*, *49*, 103990.

[4] Cabaleiro, M., Lindenbergh, R., Gard, W. F., Arias, P., & Van de Kuilen, J. W. G. (2017). Algorithm for automatic detection and analysis of cracks in timber beams from LiDAR data. *Construction and Building Materials*, *130*, 41-53.

[5] Liu, H., Wu, Y., Li, A., & Deng, Y. (2024). Precision detection and identification method for apparent damage in timber components of historic buildings based on portable LiDAR equipment. *Journal of Building Engineering*, *98*, 111050.

[6] Santos, D., Sousa, H. S., Cabaleiro, M., & Branco, J. M. (2023). HBIM application in historic timber structures: a systematic review. *International Journal of Architectural Heritage*, *17*(8), 1331-1347.

structures. Furthermore, while LiDAR excels in capturing external geometries, it is limited in detecting internal defects. Complementary techniques are often required to provide a more comprehensive assessment of timber elements.

3.1.2. Ground Penetrating Radar

Ground Penetrating Radar (GPR) is a widely used non-destructive testing (NDT) tool with applications in concrete buildings and structures scanning, bridge decks and road scanning, utility mapping, geology/geotechnical applications, archaeology, forensics, UXO detection and others[7]. GPR can detect hidden objects in a structure but also characterize and assess the condition of a material. Although not as popular as concrete and soil applications, research and commercial usage of GPR for wood and timber structures can be found and is a growing field. GPR has been used for inspecting tree trunks, wooden utility poles and other wooden structures for identifying internal cracks, knots, hidden bolts and moisture content and overall characterize the condition and strength of the wood[8].

Since its first use in the 1970s, GPR technology has advanced significantly. Improvements in antenna design, computing power, and signal processing have enhanced depth penetration, resolution, and portability. High-frequency antennas, such as the Proceq GP8800, have been developed that have a high resolution and can resolve small features while scanning building walls and floors which do not require great penetration. These probes are small, lightweight and portable that can be controlled via a tablet wirelessly and allow for in-situ real-time data visualization and interpretation. Modern commercial units are can also be handheld or cart-based and often integrated with GNSS or total stations for precise positioning. Better antenna shielding has also minimized external interference. Recently, stepped-frequency continuous-wave (SFCW) systems have emerged, supplementing the traditionally pulsed GPR technology.

Technological innovations have enabled rapid data acquisition and processing with advanced data visualization, such as 3D view and augmented reality, being available during the survey, straight after data collection. Data storage in the cloud is provided that ensures no loss of data and enables easy data sharing.

Alongside single-channel systems, multichannel GPRs have become available, mounted on carts or vehicles and equipped with multiple antennas. These enable large-scale data collection over long distances with fewer passes, reducing survey time. Wireless control,and on-site visualization tools (such as real-time depth slicing and background map integration) have further streamlined field operations.

Data collection methods vary depending on whether GPS is used. Without positioning systems, surveys require gridded layouts with parallel transects, while GPS-enabled systems allow free path movement. Data are commonly displayed as B-scans (2D radargrams with depth vs. distance) or as time/depth slices compiled from multiple scans. Basic processing can be performed during acquisition, but more advanced analysis requires dedicated post-processing software.

Beyond hardware, progress in data processing has introduced advanced signal analysis techniques, including 3D and reverse-time migration, full waveform inversion, and wavelet analysis. AI applications, such as automated rebar detection, are also being integrated. Furthermore, fully 3D electromagnetic (EM) modelling algorithms that have been developed in recent years allow for simulating antenna systems, complex materials and objects with a

[7] Daniels, D. J. (2004). Ground penetrating radar 2nd edition. *The Institution of Engineering and Technology*

[8] Rodrigues, B. P., Senalik, C. A., Wu, X., & Wacker, J. (2021). Use of Ground Penetrating Radar in the Evaluation of Wood Structures: A Review. In *Forests*.

high degree of accuracy[9]. This way, real scenarios can be modelled and the EM wave propagation through materials can be studied and assist in data interpretation. Generated modelled data are also highly used for training machine learning (ML) algorithms for automated data interpretation[10].

Although GPR has been utilised for assessing timber structures, it has certain limitations. GPR requires a dielectric contrast between different materials to exist in order to be detectable. Wood has a low dielectric constant/relative permittivity value, which often can be similar to the dielectric constant of air or of other layers (such as an insulation layer) in a wall, which can lead to weak signals from interfaces between materials and thus make the hidden object detection harder. Furthermore, irregularities in the wood surface that do not allow for a direct contact between the probe and the surface (air gaps) as well as small variations in material properties can introduce noise in the data and affect the interpretation. Also, the size of a hidden object and the thickness of a layer can pose a limitation as each probe has a limit on the smallest size that can be detected.

3.1.3. Active hyperspectral sensing

Hyperspectral imaging (HSI) and spectroscopy based on near-infrared (NIR) radiation has been used extensively for both classification of types and quality assessment of timber[11,12]. However, existing HSI devices are not suitable for on-site measurements due to their dependence on ambient light. State-of-the-art HSI acquire rely on either sunlight or halogen lamps for illumination of the target material. Hyperspectral images acquired with both light sources are prone to fluctuations due to ambient conditions. Active hyperspectral sensing (AHS) overcomes this issue by introducing a novel type of illumination, which is virtually unaffected by ambient conditions.

Active hyperspectral sensing uses supercontinuum lasers (SC) as light source. A supercontinuum laser is a light source that combines that properties of a laser (high brightness, directionality, coherence) with the broad spectral bandwidth of a lamp or sunlight[13]. Typical SC lasers used for AHS are pulsed at specific frequencies, which allows for selective detection of the reflected light, making AHS less sensitive to ambient light fluctuations.

To our knowledge, the deployment of AHS in SUM4Re is the first implementation of a hyperspectral device for standoff scan of construction materials.

3.1.4. Infrared thermography and dielectric moisture sensing

As the properties of wood and wood-based materials depend strongly on the temperature and moisture content of the material, additional measurements were used to analyse the material state at the time of AHS measurement. The purpose of the measurement is to provide context to the AHS calibration, and therefore it is not planned to be used Infrared thermography (IRT) detects infrared radiation to measure emitted heat from the objects. It is already well-tested state-of-the-art method implemented for instance in thermal imaging cameras. These cameras convert the energy in the far infrared wavelength into a visible light display.

---

[9] Warren, C., Giannopoulos, A., & Giannakis, I. (2016). gprMax: Open source software to simulate electromagnetic wave propagation for Ground Penetrating Radar. In *Computer Physics Communications*, 209, 163-170

[10] Patsia, O., Giannopoulos, A. & Giannakis, I. (2023). Background Removal, Velocity Estimation, and Reverse-Time Migration: A Complete GPR Processing Pipeline Based on Machine Learning. In *IEEE Transactions on Geoscience and Remote Sensing*, vol. 61, 1-11.

[11] Jochemsen, A., Alfredsen, G., Burud, I. (2022). Hyperspectral imaging as a tool for profiling basidiomycete decay of *Pinus sylvestris L.* In *International Biodeterioration & Biodegradation* 174, 105464.

[12] Leinonen, A., Harju, A.M., Venäläinen, M., Saranpää, P., Laakso, T. (2008). FT-NIR spectroscopy in predicting the decay resistance related characteristics of solid Scots pine (*Pinus sylvestris L.*) heartwood. In *Holzforschung*, 62, 284-288,

[13] Kääriäinen, T. Jaanson, A. V., Mannila, R., Manninen, A. (2019). Active Hyperspectral Sensor Based on MEMS Fabry-Pérot Interferometer. In *Sensors*, 19, 2192.

Dielectric moisture sensing (DMS) is a non-invasive measurement of the moisture content in a material by assessing its dielectric constant or permittivity. DMS sensors emit electromagnetic waves into the material, such as soil, and analyse the reflected signals or frequency shifts caused by changes in the dielectric properties, which are directly affected by the amount of water present. This method allows for accurate, real-time moisture monitoring.

IRT and DMS were used as a complementary measurement to provide temperature and moisture range and distribution on the measured surface to study its effect on the AHS measurement.

3.2. Equipment technical specification

3.2.1. AR iMMS-RGB

The device used for data collection was the Microsoft HoloLens 2, where specific software was developed and implemented to capture the 3D environment, position virtual markers, and take referenced RGB photos. However, Microsoft does not provide technical specifications for this device, beyond indicating that it has a range of 5 m and a battery life of 2 hours. It was necessary to perform a performance analysis to determine the limits of the AR glasses in different light and atmospheric conditions (more information in Deliverable D2.1). The HoloLens 2 integrates various sensors necessary for data collection, such as a depth sensor (Time of Flight (ToF) LiDAR), an RGB camera, four cameras for hand tracking, and an inertial measurement unit (IMU). Figure 5a shows an image of the HoloLens 2.

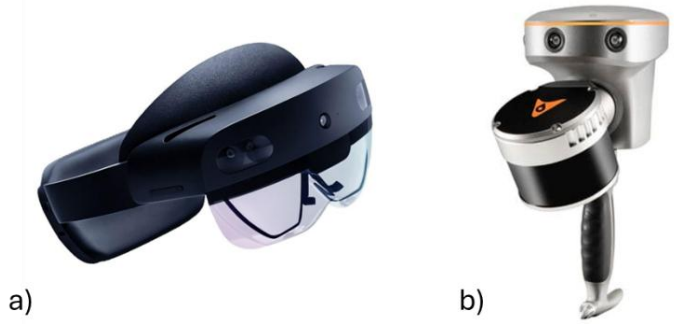

Figure 5. Microsoft HoloLens 2 (a) and CHCNAV RS10 (b)

In addition, a Handheld Mobile Laser Scanner (HMLS) CHCNAV RS10 was used to obtain reference data in the evaluation of the quality of the point clouds generated by the HoloLens 2. The technical specifications of this device are shown in Table 3. An image of the CHCNAV RS10 is shown in Figure 5b.

Table 3. CHCNAV RS10 technical specifications

Resolution	0.18º
Accuracy	10 mm
Range	0.5 to 120 m
Battery duration	1 h
Feld of View	360º vertical x 270º horizontal
Measurement rate	320,000 points per second
Operating Temperature	-20°C to +50°C

3.2.2. AHS

The technical parameters of the active hyperspectral sensor deployed in this pilot test are summarized in Table 4. The sensor operates using a supercontinuum laser emitting in the near infrared region of the spectrum, with a peak wavelength at 1550 nm due to the pump laser. The usable spectrum ranges from 1300 to 1700 nm. The spectral tuning is realized by tuning the microelectromechanical Fabry-Perot interferometer (MEMS-FPI), which filters one wavelength at a time with a full width at half maximum (FWHM) of approximately 15-20 nm. The AHS is optimized to operate at 1.5 m distance from the target. The reflected light from the target is detected by a linear sensor array, and the 2D image is acquired by scanning the target across a direction perpendicular to the line detector. In the pilot test, this scan is done by means of a rotating mirror.

Table 4. Technical parameters of the AHS

Image or drawing of the scanner:	
Size:	245mm x 229mm x 75mm
Weight:	3.2 kg (+2.5 kg of tripod)
Placement method:	Mounted on a tripod
Resistance to weather conditions:	IP63 (dust-tight, protected against sprays of water)
Other properties to take into account:	No batteries or on-device control unit in current prototype. External electrical power required for AHS device as well as for laptop for control. Operates with class IV laser. Laser safety goggles should be provided to personnel/others in the area. If the area to be scanned is normally used by people without training in laser safety (e.g. a school, a busy street pavement), it should be evacuated for the measurements.

3.2.3. GPR

The GP8800 GPR system is a step-frequency continuous-wave (SFCW) GPR transducer with a modulated frequency range of 400–6000 MHz. This is a high-frequency GPR antenna with high resolution and a maximum penetration depth of approximately 65 cm. Both the transmitter Tx and receiver Rx are included in a single enclosure. The dimensions of this probe are 8.9 x 8.9 x 7.6 cm and its weight is ~500 gr and can be operated at temperatures between 5° and 40°. The GP8800 system is equipped with an adjustable wheel, which enables scanning with both normal and cross-polarization modes. Each polarization mode can facilitate detecting different targets better than the other. The device is further equipped with a replaceable skid plate used for protecting from damage.

The GP8800 probe is powered by a removable Lithium-ion battery pack with 8h autonomy, a removable pack of 4 AA (NiMH) batteries or using an off-the-shelf 10'000 mAh power bank. It is controlled using an iPad via an application called GP app. Connectivity between the two is established via Wi-Fi or via a USB-C cable. Apart from data collection, data visualization and basic data processing can be performed though the GP app. When an internet connection is

available, the acquired data are uploaded from the iPad to the cloud, to our platform called Workspace.

This particular antenna has been designed to operate in direct contact with the ground or a material surface in order to maximize the penetration depth. Its main application is reinforced concrete scanning to pinpoint structure elements such as reinforcing bars, conduits, post-tension cables and for concrete assessment, however it is also being used for the inspection of wooden utility poles. This transducer along with some of its features annotated is illustrated in Figure 6.

Figure 6. The Proceq GP8800 transducer along with some of its features annotated

Table 5 summarizes some of the key technical specifications of the GP8800 probe.

Table 5. Technical specifications of the GP8800 GPR sensor

Feature	GP8800
Radar technology	SFCW GPR system
Modulated frequency range	400 – 6000 MHz
Penetration depth	65 cm
Dimensions	8.9 x 8.9 x 7.6 cm
Weight	~500 gr
Charging	Li-ion Battery Pack: Up to 8h Battery Pack (4xAA NiMH): Up to 2.5h Power bank (not included): Up to 8h

3.2.4. Infrared thermography and dielectric moisture sensing

Fluke Ti10 Thermal Imager (Figure 7, Table 6) was used to collect information about the surface temperature. It is widely used industrial-grade thermal imaging camera with 160 x 120 focal plane array, uncooled microbolometer and range from 20°C to +250°C. It is designed for predictive maintenance, troubleshooting, and verification in harsh environments. Its main drawback is fixed emissivity setting to 0.95, which is acceptable for the common material surfaces excepting shiny metals.

Figure 7. Fluke Ti10 Thermal Imager (picture credits: Fluke Corporation)

Table 6. Fluke Ti10 Thermal Imager technical specifications

Temperature measurement range (not calibrated below -10°C)	-20°C to +250°C (-4°F to + 482°F)
Temperature measurement accuracy	±2°C or 2% (at 25°C nominal, whichever is greater)
Field of view	23° x 17°
Spatial resolution (IFOV)	2.5 mRad
Minimum focus distance	Thermal lens: 15 cm (6 in) Visible (visual) light lens: 46 cm (18 in)
Focus	Manual
Image frequency	9 Hz refresh rate
Detector type	160 x 120 focal plane array, uncooled microbolometer
Infrared lens type	20 mm F = 0.8 lens
Thermal sensitivity (NETD)	≤ 0.13°C at 30°C target temp. (130 mK)
Infrared spectral band	7.5 µm to 14 µm
Visual camera	640 x 480 resolution

FLIR MR60 Moisture Meter Pro (Figure 8, Table 7) was used to collect the information about the material moisture. It is a dual-function, handheld instrument designed for quantitative and qualitative moisture analysis in a wide range of materials. It integrates both pin-based (resistive) and pinless (dielectric) measurement technologies, allowing for destructive and non-destructive testing, respectively.

Figure 8. FLIR MR60 Moisture Meter Pro (picture credits: Teledyne FLIR)

Table 7. FLIR MR60 Moisture Meter Pro technical specifications (dielectric pinless mode)

Measurement Resolution	0.1
Moisture Depth	1.9 cm maximum
Moisture Range	0–100 relative measurement
Response Time	100 ms
Sample Rate	10 Hz
Operating Humidity	≤ 90%, 0~30°C, ≤ 75%, 30~40°C, ≤ 45%, 40~50°C

3.3. Equipment description with respect to application and utilization

3.3.1. AR iMMS-RGB Scan

HoloLens 2 were not designed specifically to capture 3D data, but rather for Mixed Reality, where priority is given to the constant (real-time) updating of the nearby 3D environment for interaction. Considering that the 3D data generated will be used for material identification and C-BIM generation, the methodology designed has significant limitations compared to conventional devices:

1. The range of the LiDAR sensor is up to 5 m according to the datasheet, but empirical tests have reported a useful range of up to 3 m. Conventional LiDAR for capturing interiors can have ranges of up to 30 m or 100 m. The range limitation means that elevated areas that are not accessible cannot be scanned and that the data collection trajectory must be closer to the objects.
2. Lower data resolution (point density) makes it difficult to detect complex objects, making it impossible to detect small elements.

On the contrary, Mixed Reality options allow us to take advantage of technology:

1. Data collection is updated and visualized in real time, so errors (occlusions and scanning of uninteresting dynamic objects) can be identified onsite and corrected. In addition, constant refreshing generates a more uniform point density.
2. The device is not only a capture sensor, but also acts as a computer, so software and functions can be implemented to process data and interact with the scanned virtual environment.
3. Virtual markers placed during scanning allow objects of interest to be identified more easily, thus improving subsequent automatic detection.

Each sensor operates differently for each data collection. HoloLens 2 generates several point clouds measuring approximately in a 5 m radius sphere, which are then exported and joined together to generate a complete point cloud of the study area. The RS10 generates a single point cloud for each data collection. All point clouds generated are georeferenced and registered with each other to ensure spatial consistency between sensors.

3.3.2. AHS

Applied to detect surface damage and assess timber conditions. The data collected with the AHS contains information about the surface of the material, since the NIR radiation has a shallow penetration depth (few mm). This means that, if there is any coating or painting on the wood, it will likely affect the spectra (provided the coating/paint is not transparent in the NIR region).

The spectra collected with AHS corresponds to material fingerprints, as the spectral features are related to specific molecular and intermolecular bonds of the analysed material. In the case of solids, such as wood, the intermolecular bonds may reflect physical properties of the material (e.g. density) which may be affected by aging or deterioration.

The AHS is particularly sensitive to moisture due to an absorption band of water around 1420 nm. In addition, the NIR spectrum also presents features related to the main components of timber, namely cellulose, hemicellulose and lignin. The proportion of these different components, as well as how they are structurally organized in the material are specific to each type of wood, as well as their conditions. For example, different types of mould selectively decompose the different wood components, rendering specific spectral signatures.

Therefore, we can enumerate the following expected parameters to be assessed with AHS in the pilot test:

1. Type of wood
2. Coatings/paintings, and their possible conditions.
3. Moisture
4. Presence/type of mould

It is important to note that what kind of information can be retrieved from the list above depends on the availability/quality of training data. In the case of the Svalbard pilot test, we have generated databases related to the presence of mould, moisture and type of wood. More details of this database can be found in Deliverable 2.2.

3.3.3. Infrared thermography and dielectric moisture sensing

Fluke Ti10 Thermal Imager was used to capture temperature distribution of the areas scanned by AHS. If the surface was in direct sunlight a complementary measurement was made later when the surface was not exposed. FLIR MR60 Moisture Meter Pro was used in dielectric (pinless) non-destructive mode to preserve the value and surface integrity of the potentially reusable material. Measurements were made in corners of the areas scanned by AHS or on each plank of the wooden fence.

3.3.4. GPR

The GP8800 system, although initially designed for reinforced concrete scanning, it can be used to other materials and applications that need high resolution and require a small

penetration depth. Wooden materials can be scanned and penetrated with GPR with applications such as wooden utility pole scanning found.

For this specific application, GPR can be utilised to detect hidden structural components inside the walls and floors (such as wooden studs, beams and joints, metallic and non-metallic objects), detect voids, detect the different layers inside of walls/floors (e.g. insulation layer) and assess their condition. Condition assessment involves evaluating the presence/continuity of e.g. insulation layers, moisture detection and finding defects. In addition, depths of targets and thickness of layers can be estimated. Since walls and floors are of small thickness, the maximum penetration depth of the chosen system is sufficient.

Since this is an NDT technique, it allows for inspection without removing the cladding or other components.

In contrast, the ECT sensor cannot be used for this application as it is based on electromagnetic induction and is necessary for conductive materials, most commonly metallic rebars, to be present.

Since GPR can penetrate timber, it can be useful in linking visible/surface damage with subsurface deterioration. In certain cases, the extent of visible surface cracks to the internal structure can be determined from GPR reflections from voids/fractures inside the timber. In addition, areas of surface discoloration and staining could be related to GPR signals that indicate increased moisture content inside the timber structure as moisture affects the EM wave propagation. Furthermore, warped or uneven timber surfaces can also be correlated with internal anomalies detected by GPR. With dense high-resolution data collection and accurate data positioning, small features such as voids could be detected. However, if an internal crack will be detected depends on the resolution of the antenna used (very high-resolution in this case), the size and depth of the crack and the surrounding material conditions. Also, small vertical cracks are difficult to detect with GPR.

3.4. Preparatory measures

This section describes any required preparatory actions to the actual AHS and GPR on-site measurements. No preparatory measurements were needed for AR iMMS-RGB Scan IRT. Also, for DMS measurements no preparatory actions were required, because the off-shelf equipment was used to obtain only complementary data to AHS.

3.4.1. AHS

To extract qualitative or quantitative data from hyperspectral images or spectra, we need to obtain relevant databases for a given application. This is because any given spectrum typically comprises a convolution of multiple features from all the components of a material, and therefore, interpreting this data by itself would require applying complex theoretical calculations. Typically, such theoretical approach is only possible for simple laboratory systems consisting of pure substances. Thus, any analysis of real samples relies on training/calibration using databases acquired with the same equipment.

In the case of the Svalbard pilot test, we acquired the training data by scanning wood samples (25 mm diameter disks) from the pilot site in the VTT laboratory prior to the field test. We scanned the samples both with AHS and a conventional state-of-the-art hyperspectral camera. We measured the wood samples as they arrived, and also after treatment in 95% humidity chamber.

Figure 9 shows photos of the samples, as well as preliminary cluster analysis based on Uniform manifold approximation and projection (UMAP). More detailed explanations regarding the calibration data acquisition and analysis will be given in deliverables D2.2 and D3.2.

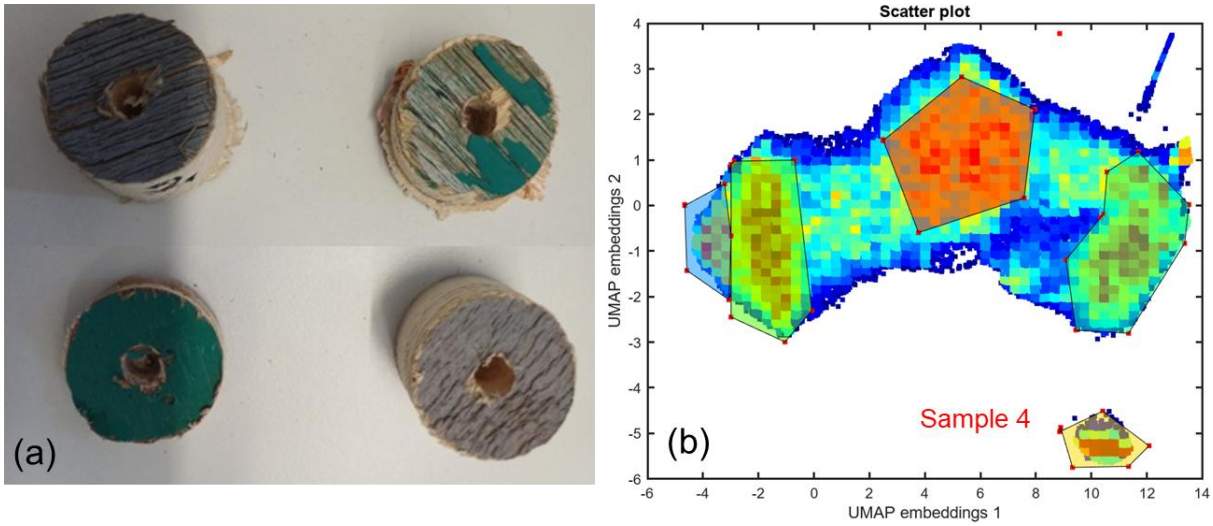

Figure 9. Wood samples analysed in the VTT laboratory with AHS and conventional HIS prior to the pilot test. (a) Sample photos; (b) UMAP analysis scatter plot.

3.4.2. GPR

A mock-up of the pilot wall shown in Figure 10 was built and scanned with GPR prior to the testing in Svalbard in order to assess what information we can extract using GPR in this type of structures. The results from the mock-up will also help with the interpretation of the data from Svalbard. The sample has dimensions of 1200 × 800 × 211 mm and consists of different layers as seen in Figure 11.

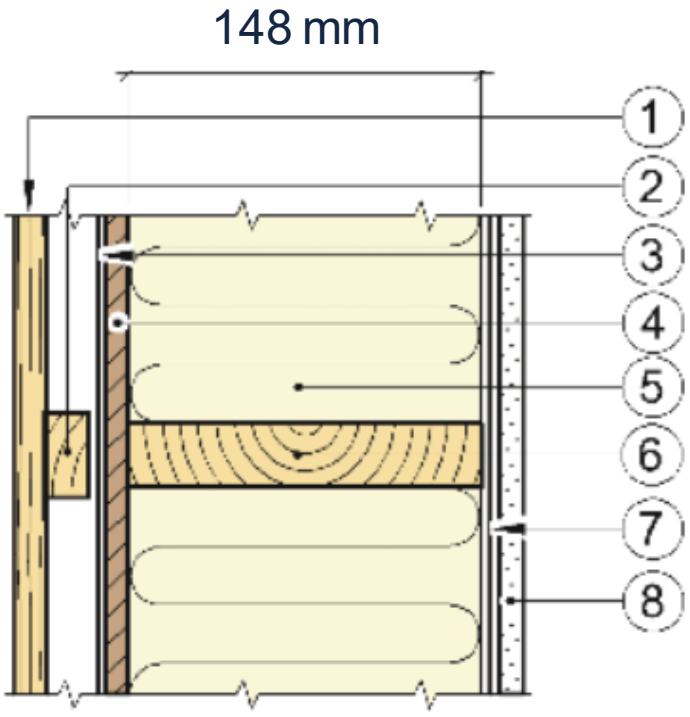

Figure 10. Horizontal section view of pilot outer wall with material composition [14]

[14] 1) 19x148 mm horizontal double-beveled cladding with two layer of system coat; 2) 23x48 mm battens/ventilation c/c 600 mm; 3) Wind barrier; 4) 12 mm windproof asphalt panels; 5a) 150 mm glass wool insulation; 5b) 150 mm rock wool insulation; 5c) 150 mm wood fibre insulation; 6) 36x148 mm studs C24; 7) 0.15 mm plastic film/vapor barrier; 8) 9 or 11 mm medium/high density fibre board; 9a) 36x148 mm C24; 9b) 36x148 mm C24; 10) 12 mm plywood for transportation and mock-up borders.

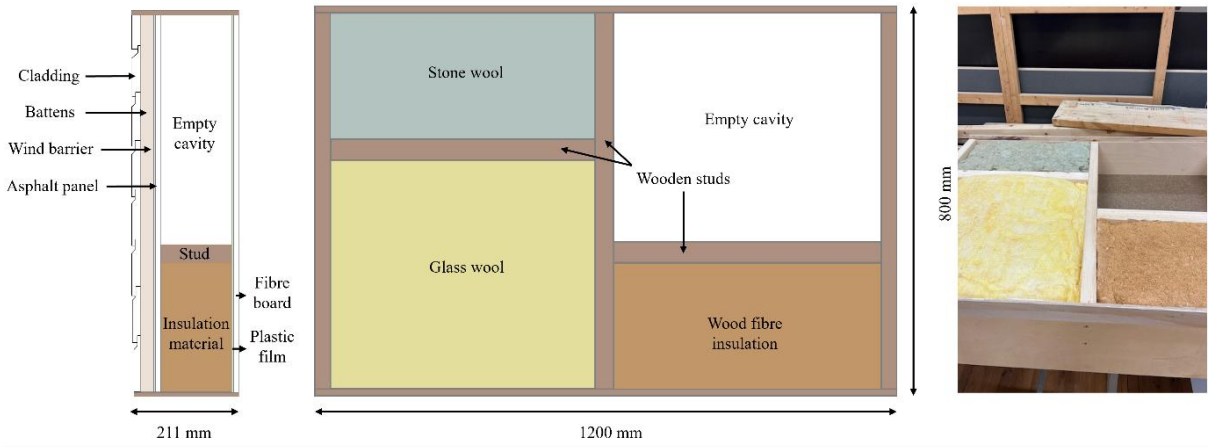

Figure 11. Structure of the mock-up wall. Left: Side view which shows the different layers, Middle: Structure of the insulated region, Right: Image of the insulated region for reference.

The sample was scanned using the high-resolution Proceq GP8800 GPR system, At first, line scan measurements were acquired to calibrate for the bulk dielectric/velocity through the medium utilising the known thickness of the specimen. The calibrated dielectric/velocity values were need as these are used for calculating the depth. As electromagnetic waves travel faster through air, a dielectric of 1.3 was estimated for the region that includes the empty cavity (as most of the wall has air), and 2.0 for the regions where insulation materials exists.

For the data acquisition on the mock-up, two area scans of 60 x 60 cm were conducted on each side (external cladding and internal side) to ensure the full mock-up is scanned, leading to a total of four area scans. In the area scans, measurements were collected with a spacing of 5 cm, both in the x and in the y direction. Therefore, in total 26 measurement lines were collected for each area scan. To mark the area and the lines, a marked grid paper was used. The area scan locations (marked with blue shade color) along with the GP8800 GPR system and the grid paper used, can be seen in Figure 12. The same locations were scanned also from the internal side. The figure also highlights with the measurements selected and presented here. The solid lines represent measurements presented from the external side and the dashed lines measurements from the internal side.

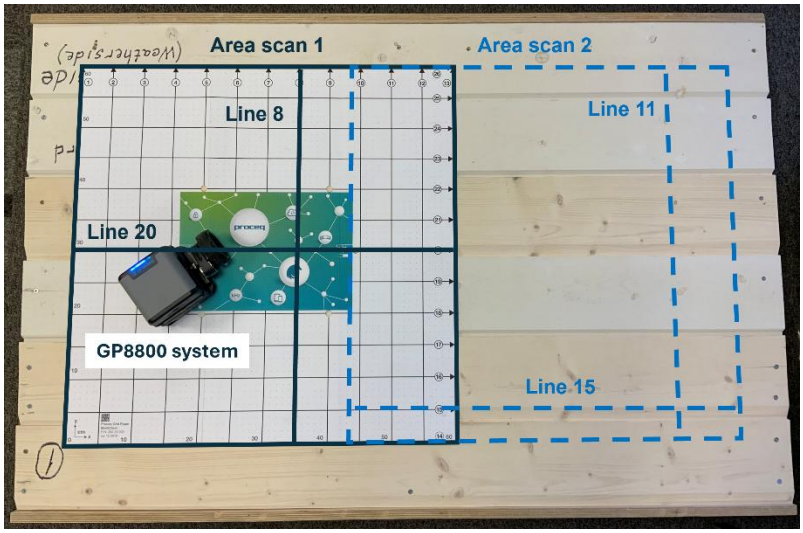

Figure 12. The area scan locations on the mock-up wall along with the GP8800 system. The solid lines represent scans from the external side, whereas the dashed lines, scans conducted from the internal side.

After the data were acquired, the following processing steps were applied in order:

1) Time zero correction: This filter is used for correct depth estimation
2) Noise cancellation filtering: Used for removing noise in the data
3) Background removal: Used to remove the response from the surface which due to being strong masks other responses.
4) Gain: Used to amplify the responses

Results

The results are presented either in the form of images, which represent a single line scan (radargram) or all the data have been combined to generate a volume from which depth slices are extracted. A depth slice from the internal scan at 12 mm depth was selected and shown in Figure 13 below. Here, the middle and wooden studs that split the insulated region in the four compartments can be identified with the depth observed in the GPR data matching their actual depth in the mock-up.

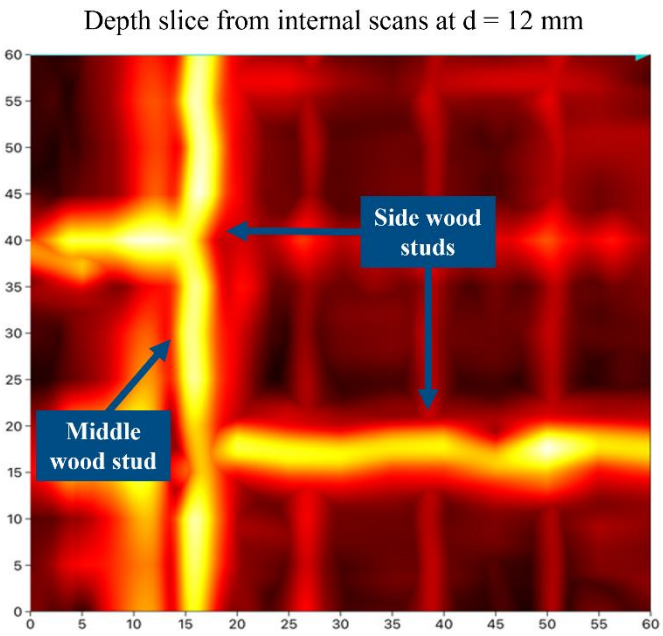

Figure 13. Depth slice at a depth of 12 mm from internal scan 2 where the wooden studs can be identified.

From the individual radargrams, more information can be extracted. In the internal scans, the response from the wood studs can be observed but also the insulation/asphalt panel interface and the cladding/air interface.

Signals from the edges of the mock-up can be seen in the data, called air waves, which are due to the finite size of the wall sample. These are expected to be minimized in the data of the much larger building wall in Svalbard. Looking at the responses from the two interfaces, we can see that these arrive slightly later and appear deeper in the left section of the Line 11 radargram (on the left of the light green dashed line). This is due to the insulation material where, as mentioned earlier, the waves travel slower than the right side, which has mostly air. Therefore, if this type of responses is identified, they could indicate potential change of material. These are illustrated in Figure 14. The gaps in the fibre board introduce noise but this does not affect the data significantly.

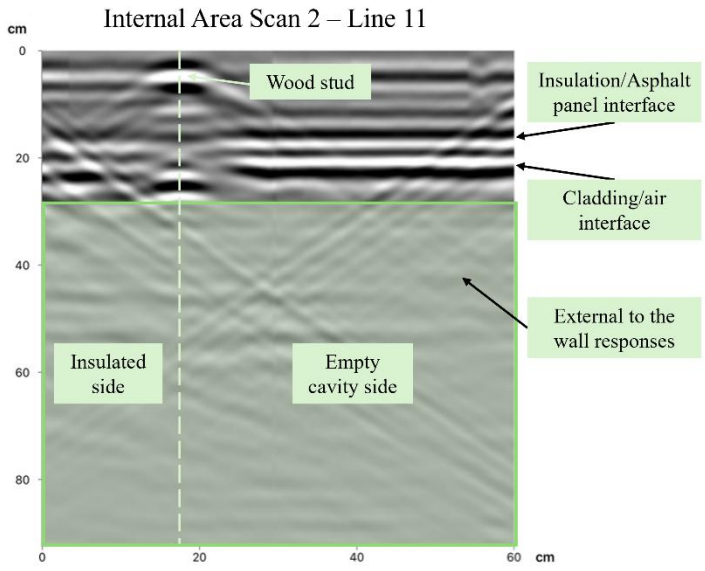

Figure 14. Line 11 radargram from internal area scan 2 with responses detected highlighted

In contrast, when scanning externally, the larger gaps and the irregularities in the external cladding surface introduce significant noise (see Figure 15). In addition to this, the metallic nails on the cladding surface due to their strong signal mask the response from the wood stud. A distinction between the wooden cladding and the wooden battens layer cannot be made from the GPR data, which was expected due to their similar dielectric properties.

Although the external scans were more challenging, more information can be extracted from the external x-directed scans, where the asphalt panel/insulation and the fibre board/air (backwall) interface can be detected. The backwall response can be used to find the wall thickness in case not known, assuming the dielectric constant is known.

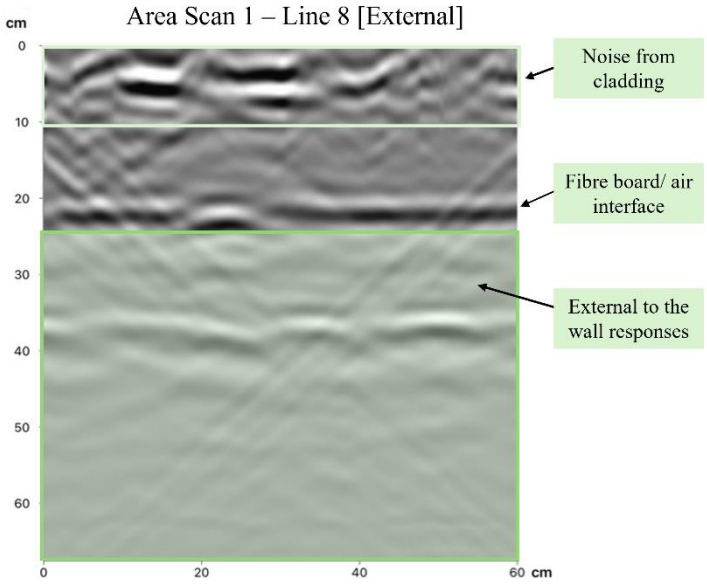

Figure 15. Line 8 radargram from external area scan 1 with responses detected highlighted

3.5. Quality assurance and control measures

3.5.1. AR iMMS-RGB

Immediately after the scans, the quality and completeness of the data is checked to assess whether repetition was necessary. The HoloLens data is exported directly from internal storage in text file format. This maximizes the compatibility across many point cloud programs. RS10 raw scan data is processed and exported using CoPre2 software. The resulting point clouds from both cases are visualized using the free Cloud Compare software.

3.5.2. AHS

The data collected using AHS is transferred to a second laptop to avoid slowing down or interrupting the scan and checked with own Matlab application for quick evaluation of the data. This quality check is to ensure that the overall image is consistent with the scanned target, and the spectra of individual pixels do not present any anomalies. An example of raw data as viewed in the Matlab application is shown in Figure 16. The right panel shows a false color image of the scan (i.e. an RGB image created from selected NIR wavelengths that are not visible in a regular photo), and the plot on the bottom left panel shows few raw spectra of selected pixels. In this software, it is possible to quickly spot if anomalies in the spectra of pixels are present, as this will distort the corresponding area of the false colour image.

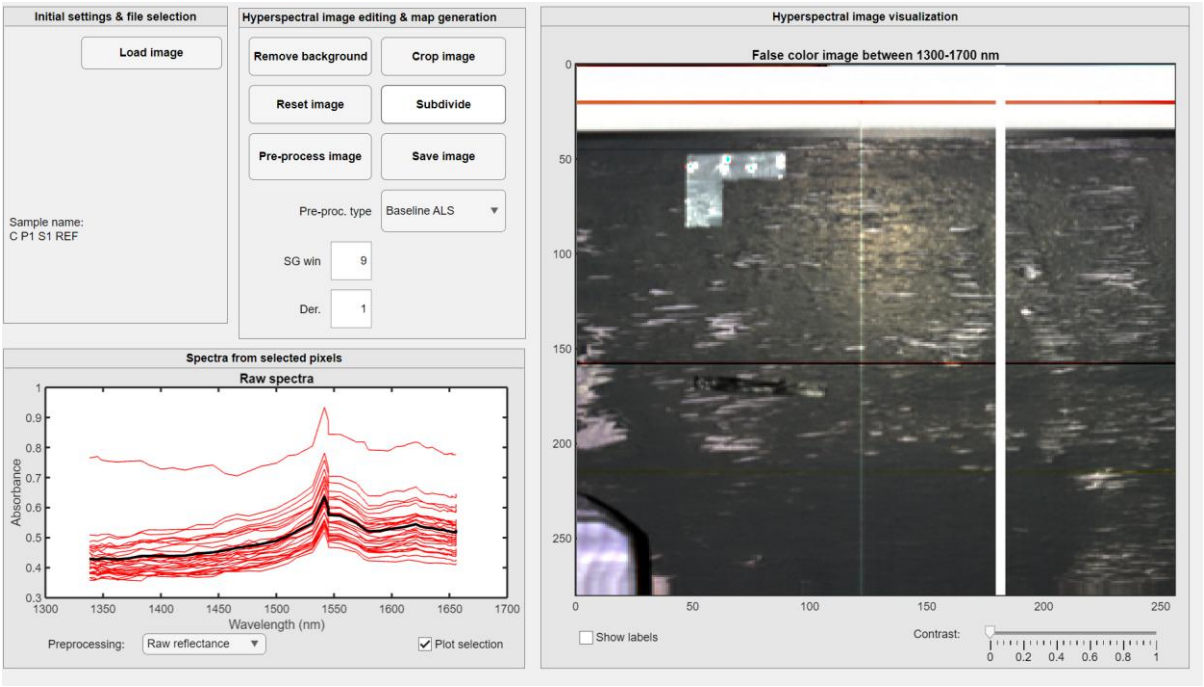

Figure 16. Screenshot of custom Matlab application for assessing the quality of AHS data

3.5.3. GPR

Two units of the GP8800 probe will be transported to the pilot site in order for a backup unit to be available in case equipment issues arise. Both units will be fully tested before Svalbard and although the battery packs are rechargeable, additional battery packs will be also carried.

As mentioned above, data visualization and quick post-processing will be made on the same day after data collection to check the quality of the collected data and that there were no other issues/errors with the data collection and survey settings. If any issues are found, a second data acquisition can be made on the following day. If there are no issues but potential areas of interest are observed, some additional scans can be made around that area. The collected data will be uploaded to the cloud but also downloaded locally as a backup.

Due to the cladding on the outer face of the wall, which has gaps between the wooden panels but also due to the cladding surface not been flat, noise could be observed in the data from the external wall scans which can make the interpretation difficult. Based on the mock-up tests, this does not affect the data significantly. However, this effect will be assessed on the actual pilot site due to variabilities that might exist between the mock-up wall and the actual building wall.

Prior to the pilot site visit, test scans on the mock-up pilot wall have been conducted but also numerical simulations of the mock-up samples. These datasets will be compared with the scans from Svalbard for checking both the quality of the measured data but also for assisting in data interpretation.

4. Data acquisition plan

The strategic plan ensures efficient execution of pilot activities through clear role assignments as well as scheduling and definition of the measurements.

4.1. Human resources assignment and roles

Each partner's role is implicitly aligned with their expertise to ensure a smooth workflow and optimal outcomes, as summarized in Table 8.

Table 8. Contributors and their roles in the Nordic pilot

	Affiliation	Role	Contact info e-post etc
Emil Lindberg	STORE NORSKE	Contact person "Nordic Pilot"	Emil.lindberg@snsk.no
Henning Stalsberg	STORE NORSKE	Head of Building Department	Henning.stalsberg@snsk.no
Sveinung Nesheim	SINTEF	Responsible of D10.3	sveinung.nesheim@sintef.no
Ramon Hingorani	SINTEF	Co-responsible of D10.3	ramon.hingorani@sintef.no
Francisco Senna Vieira	VTT	Contact person AHS	francisco.sennavieira@vtt.fi
Teemu Kääriäinen	VTT	Contact person AHS	Teemu.Kaariainen@vtt.fi
Petr Hradil	VTT	Contact person AHS	petr.hradil@vtt.fi
Jesús Balado-Frías	UVIGO	Contact person AR iMMS-RGB	jbalado@uvigo.gal
Juan Carlos Navares-Vázquez	UVIGO	Contact person AR iMMS-RGB	juancarlos.navares@uvigo.gal
Pedro Arias	UVIGO	IP	parias@uvigo.gal
Ana Sánchez	UVIGO	PM	anasanchez@uvigo.gal
Alex Novo	EAGLE	Contact person GPR	alex.novo@screeningeagle.com
Rania Patsia	EAGLE	Contact person GPR	ourania.patsia@screeningeagle.com

4.2. Measurement schedule

AHS measurements (VTT) were performed on May 28–29 2025, while both GPR (Eagle) and AR iMMS-RGB (UVigo) measurements took place on June 12–13, 2025, as summarized in Table 9.

Table 9. Testing schedule overview

	May 28th and 29th External testing (AHS)	June 12th and 13th External and internal testing (GPR, AR iMMS-RGB)
UVIGO	NA	Day 1: 6 hrs; Day 2: 4 hrs
VTT	Day 1: 8 hrs; Day 2: 4 hrs	NA
EAGLE	NA	Day 2: 8 hrs.

4.3. Positioning and definition of scanning areas

This section explains the placement and size of scanning areas to be used for AHS (executed by VTT) and GPR (executed by Eagle) scanning technologies. A system of legends is defined to aid. In the following drawings and illustrations of the scanning areas, three different positions ID labels are used: One for the positions of the timber cladding samples, and one for the positions of external and internal scanning areas (see Figure 17).

For the definition of scanning areas, a three-colour code is used: Green for AHS, red for GPR and violet for common scanning areas (AHS and GPR). Scanning areas perpendicular to the drawing plane is represented as a line. Dashed lines are used for optional scanning area positions.

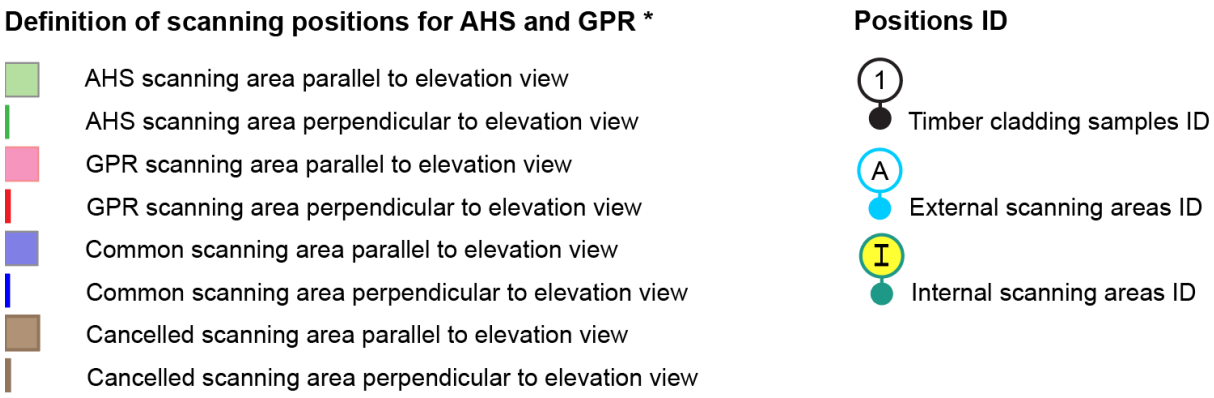

Figure 17. Definition of legends used for scanning areas information

The measurement positions are defined in the building drawings shown in Figure 18 to Figure 21 below. The positions were selected based on a combination of the pilot context, building properties, and the specific capabilities of the scanning technologies defined in the planning phase. The goal of the data acquisition campaign is to evaluate how non-destructive methods can support characterization of both visible and concealed building elements. In particular, scanning positions were chosen to:

- Capture representative façade conditions where AHS can detect moisture exposure, coating degradation, and potential biological growth typical for Arctic climate conditions.
- Access interior and balcony areas where GPR can reveal hidden construction layers, studs, and voids, supporting hidden-component mapping.

Additionally, the selection also reflects practical prerequisites such as physical access, safety, and other on-site constraints.

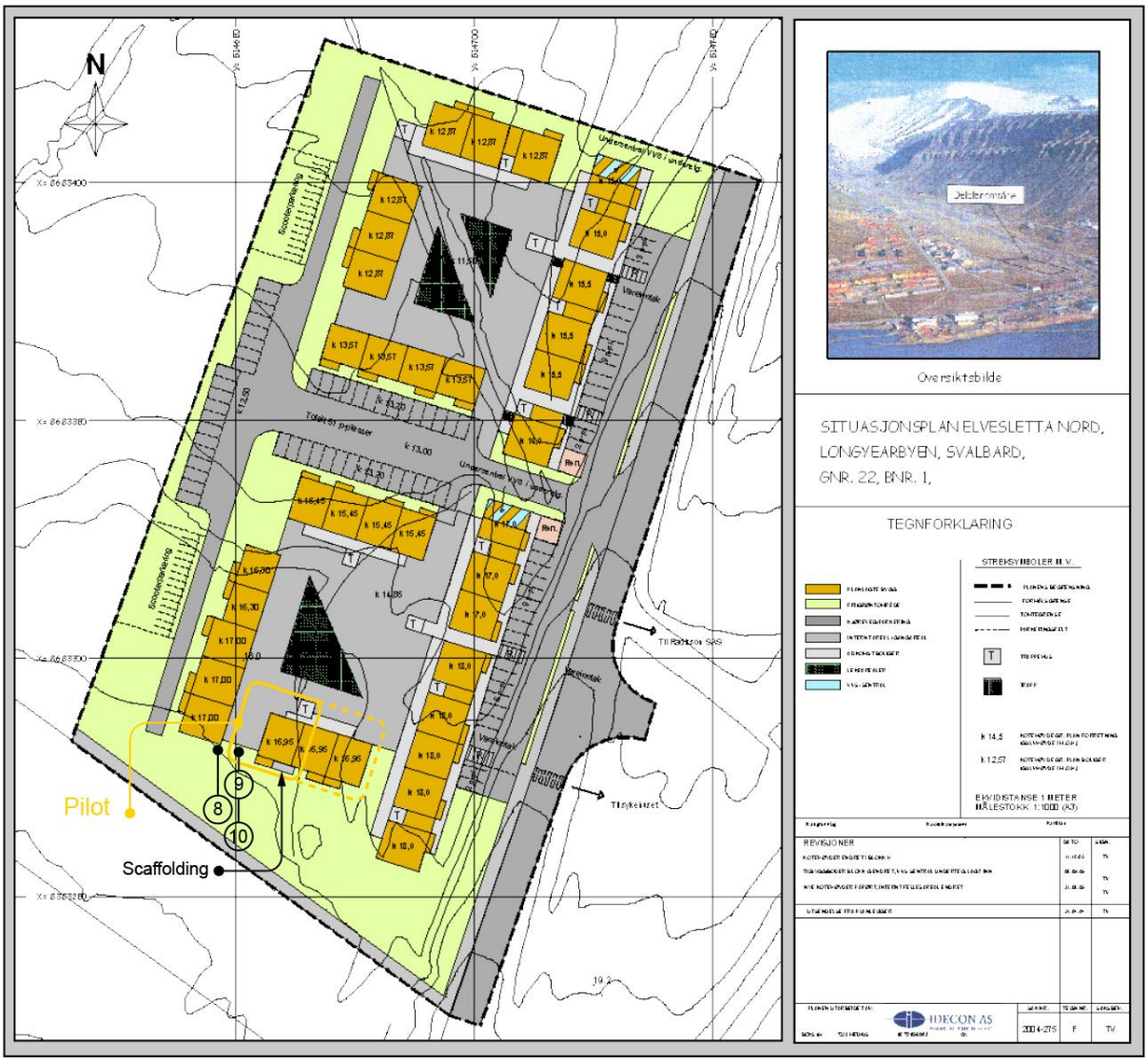

Figure 18. Situation drawing with selected scanning positions and the Nordic pilot in red border

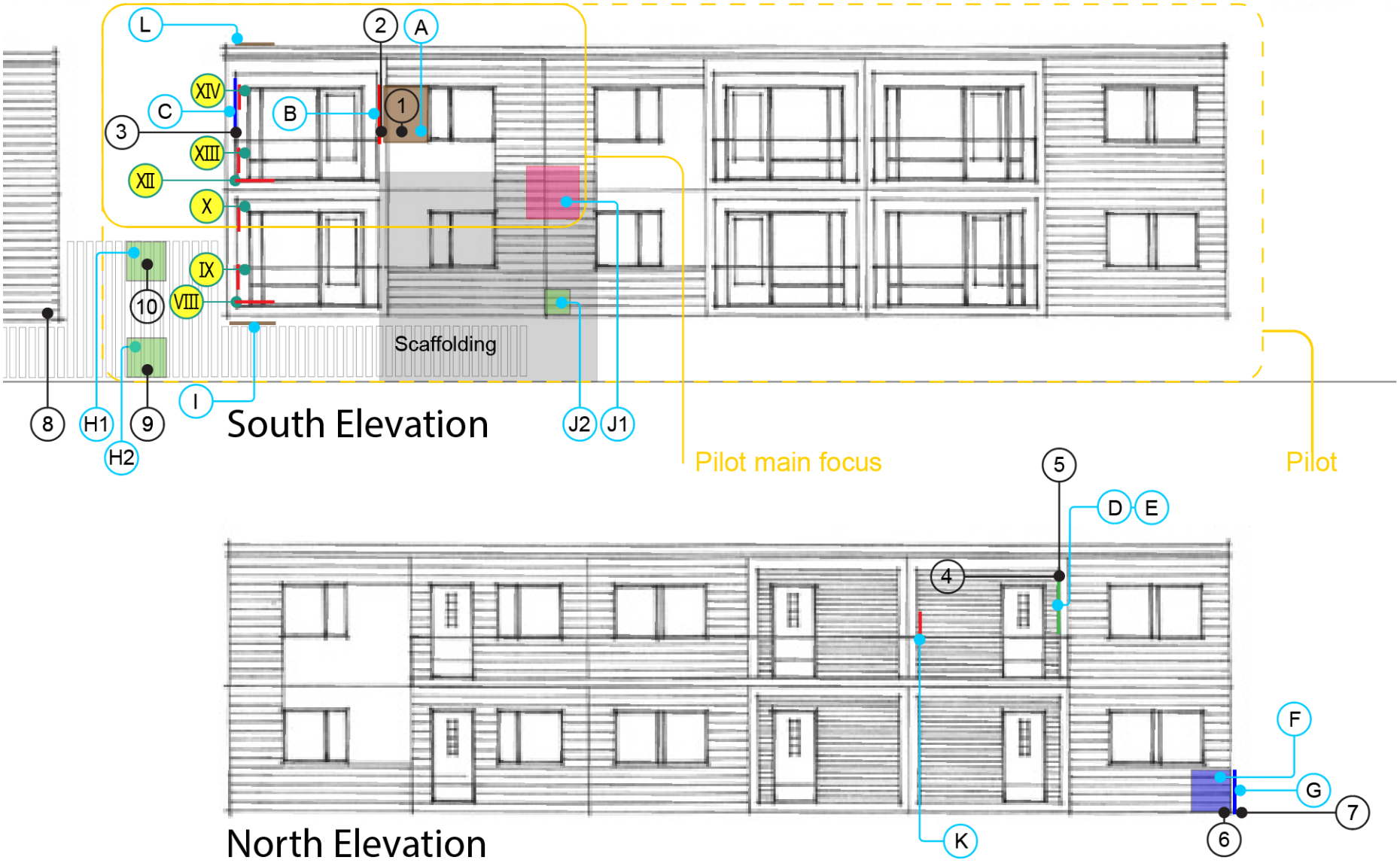

Figure 19. Elevation drawing of scanning positions

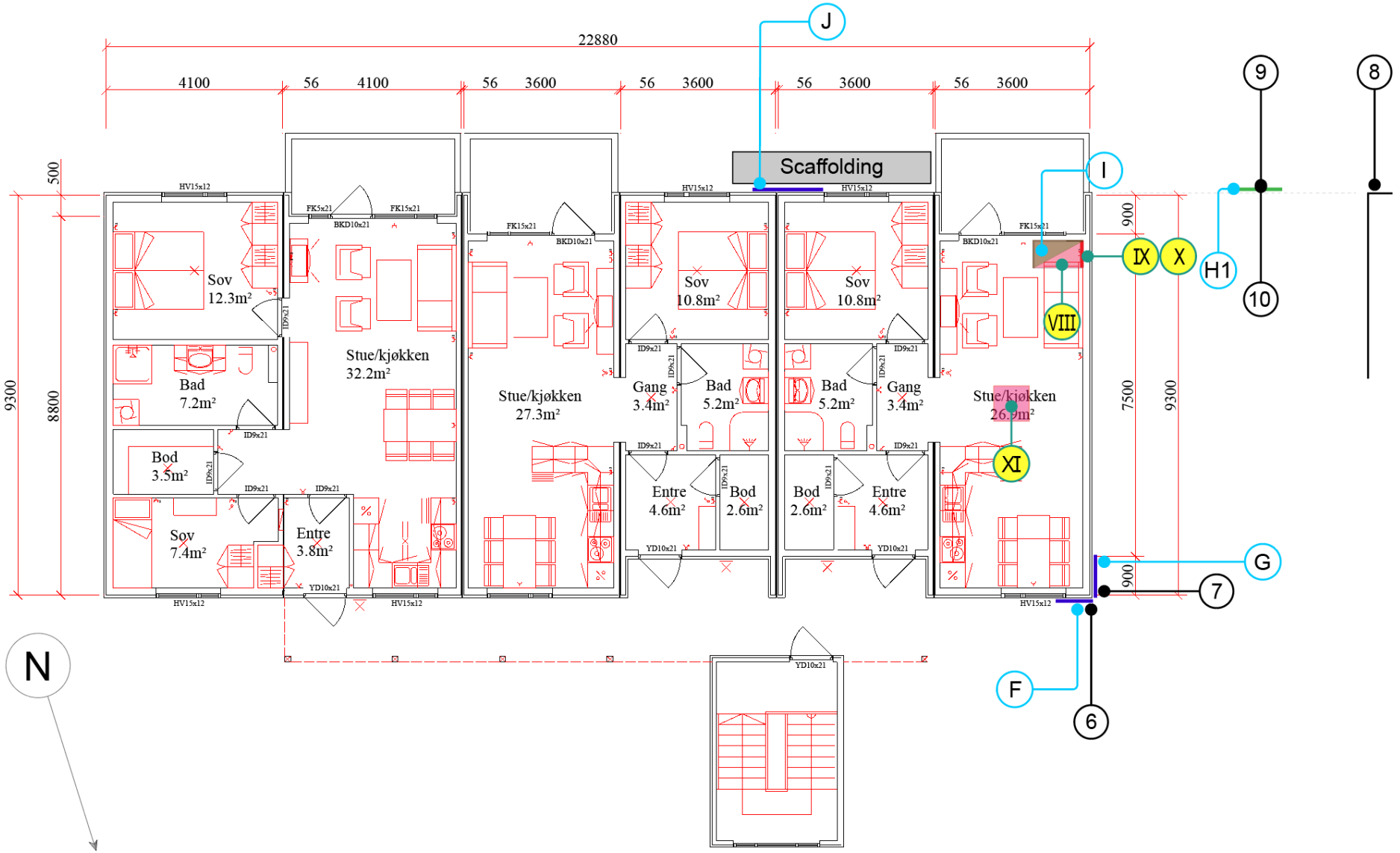

Figure 20. Plan drawing of scanning position ground floor (storey 1)

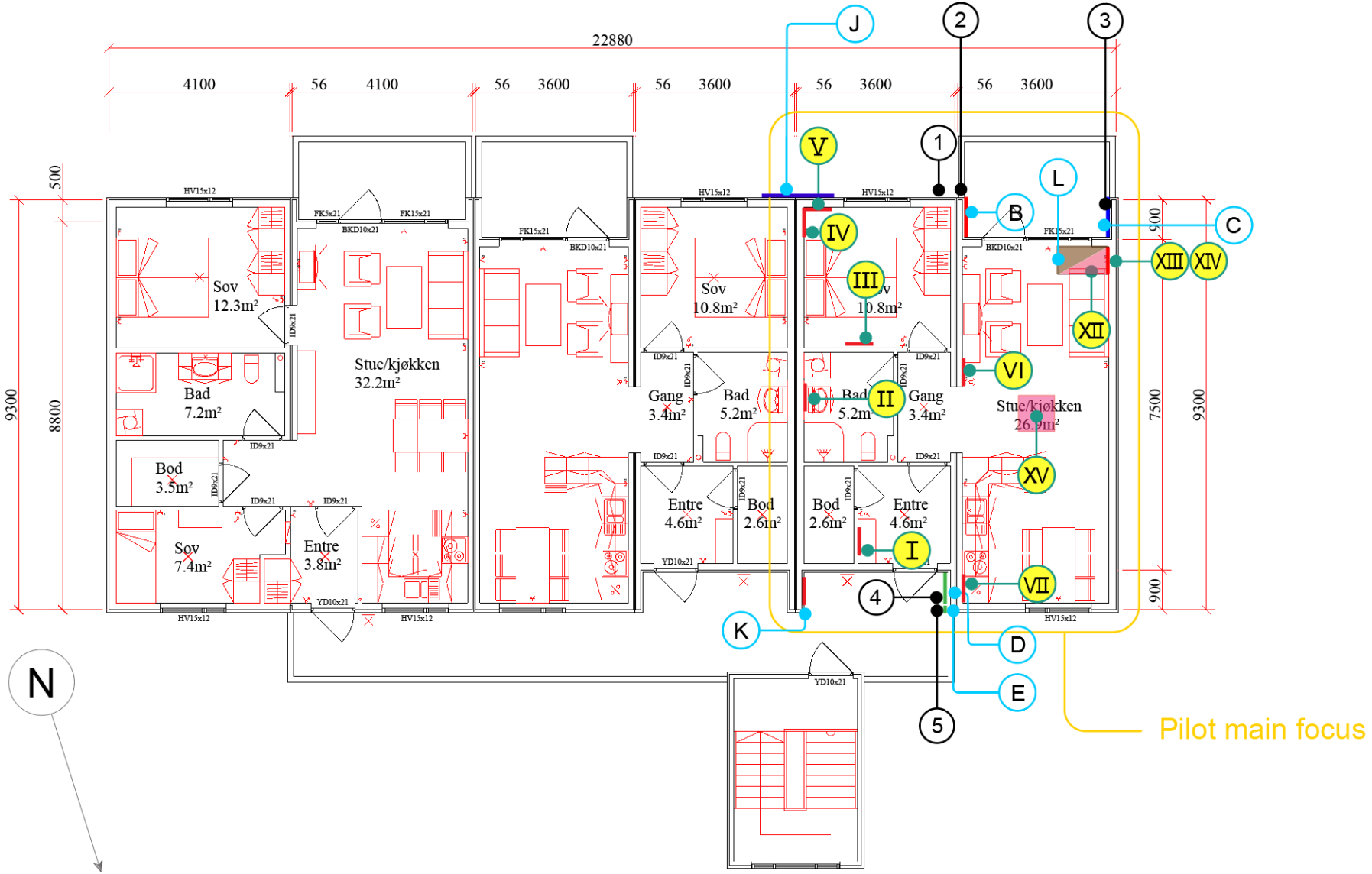

Figure 21. Plan drawing of scanning position upper floor (storey 2)

5. Implementation

5.1. Execution

5.1.1. AR iMMS-RGB Scan

Data collection with AR iMMS-RGB Scan was conducted on the afternoon of Thursday, June 12, apartment floor 2 and the exterior, while the morning of Friday, June 13, was used to scan the apartment floor 1 (and the exterior as well, to match the previous day's scan). Equipment employed was Microsoft HoloLens 2 and CHCNAV RS10, technical details on Section 3.2.1. Personnel involved were Juan Carlos Navares-Vázquez for HoloLens 2 use and Jesús Balado-Frías and Pedro Arias for RS10 use (Section 4.1). Time needed for data collection is compiled in Table 10.

Data collection was carried out partially in parallel with both devices without interfering with each other, as they were used simultaneously in different spaces. Data was collected with HoloLens 2, marking structural elements, objects of interest for recycling, and the data collection areas of AHS and GPR devices. Data collection for the apartment on floor 2 began inside and ended outside, surrounding the building in a continuous scan, while the opposite trajectory was followed for the apartment on floor 1. Images of data collection are shown in Figure 22.

Figure 22. Images of the data collection with Microsoft HoloLens 2 (a-b) and CHCNAV RS10 (c)

5.1.2. AHS

We collected data during the 28th and 29th of May, 2025. The selected areas for scanning were described in section 3.5.1.2. On the first day, there was snowfall and some scans had to be repeated. Overall, the quality of the data collected was sufficient for analysis. The AHS data collection was performed by Francisco Senna Vieira and Teemu Kääriäinen. Figure 23 shows how the AHS was setup on two locations of the pilot test.

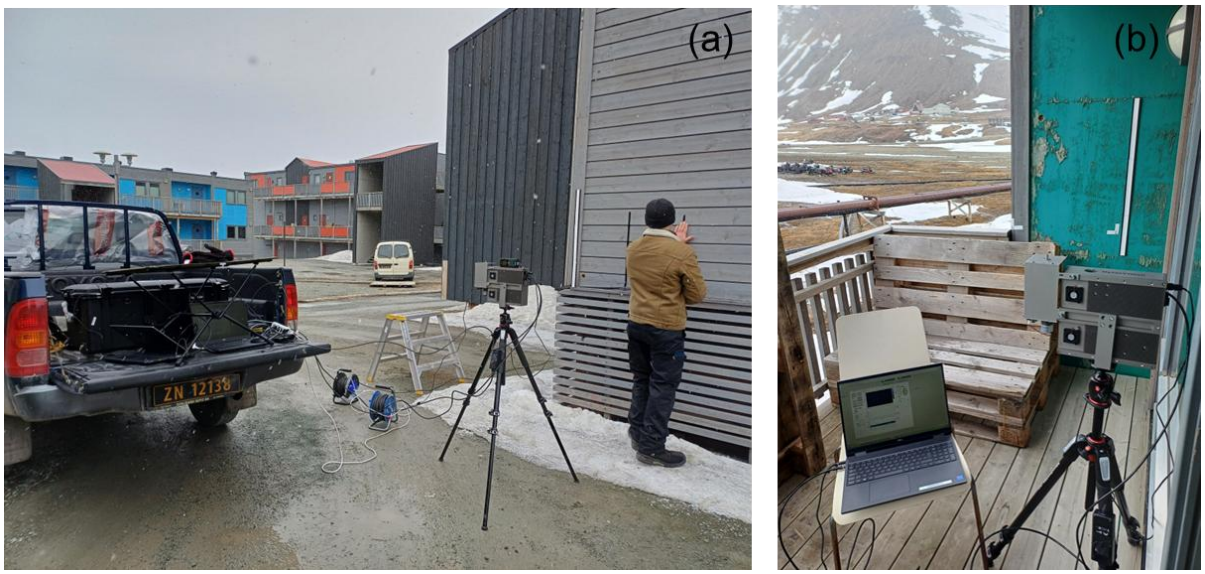

Figure 23. Setup of the AHS during the pilot test. (a) Preparation near area G and (b) setup during scan in area C.

5.1.3. Infrared thermography and dielectric moisture sensing

Temperature and moisture measurement was done the same days as AHS scanning, in particular 28.5.2025 between 15:20 and 16:35 and 29.5. between 8:50 and 12:30 (GMT+2). The goal was to localize possible moisture traps and thermal bridges that may affect the interpretation of AHS results on-site and then analyse the data further later on. The scanned areas were C, D, F, G, H1, H2, J1 and J2. It should be noted that area J2 was introduced on the second day of measurements, and the moisture scanning was not performed on this area. It is however assumed that the moisture levels were consistent across the south façade.

5.1.4. GPR

Data collection with GPR was performed on Friday, June 13, 2025. Field records from the GPR measurements are collected in APPENDIX A.

Both the first floor and second floor apartment were scanned internally, with certain scans also conducted externally where possible. For certain external scans, scaffolding was used. For scanning, the Proceq GP8800 GPR system was used, which was described in Section 3.2.3. The data collection was performed by Alex Novo and Ourania Patsia (Eagle) with assistance from Ramon Hingorani (SINTEF).

The scans were performed starting from the first-floor apartment internally, then moving to the second-floor apartment internally and finishing with the external scans. The device was controlled via the GP app and after the acquisition, the data were checked on-site to ensure there were no issues (or repeat scans if needed). Images of the data acquisition using GPR are presented in Figure 24.

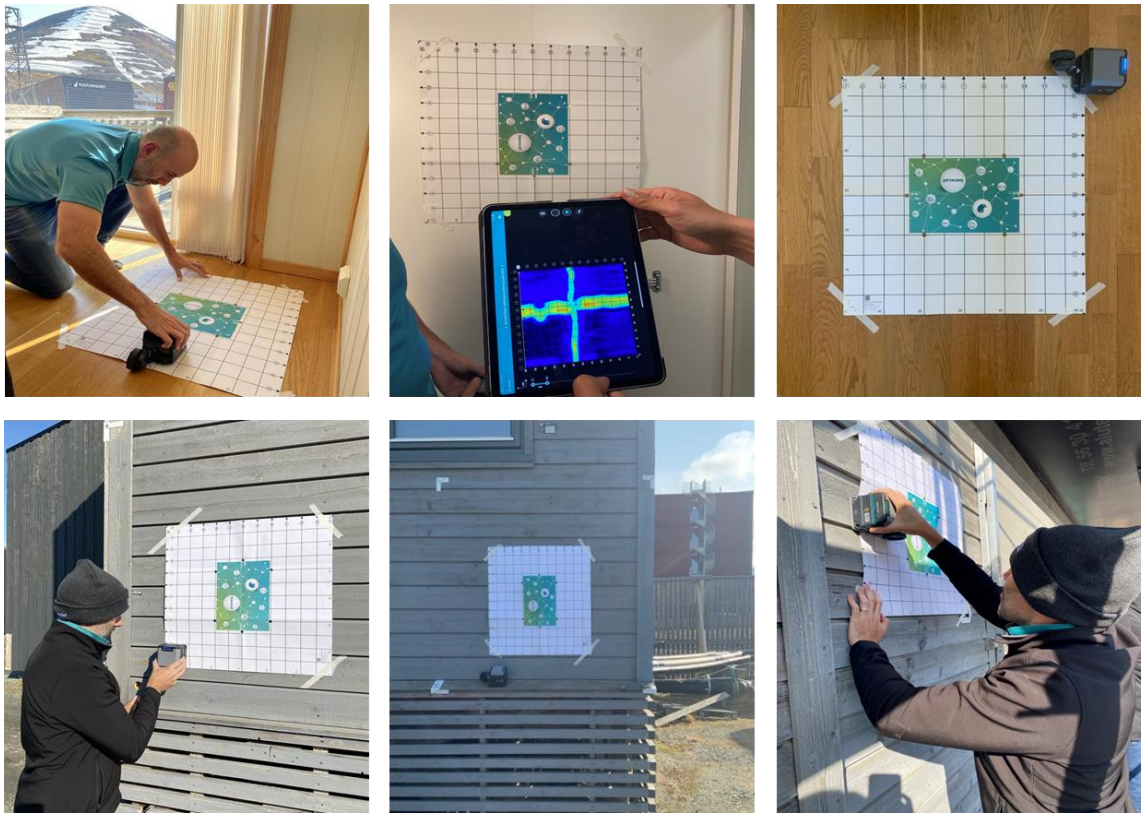

Figure 24. Photos from the GPR data collection from internal scans (top) and external scans (bottom).

In total, 24 scans were collected, out of which 21 were area scans and 3 were line scans. The line scans were collected only in some wall sections to determine if there are targets of interest or if the area differs from the rest and decide if a full area scan needs to be conducted. Measurements were conducted at multiple locations to ensure that there are datasets representative of each section of the building, namely:

- Different internal walls
- Internal wall between two apartments
- Different external walls (Scanning from the internal side)
- Floor over foundation
- Floor of second floor apartment
- On the floor of two different rooms
- On the external wall section between the first and second floor on the area between the windows of the lower and upper apartment.
- On the side wall of the balcony
- Where possible, the same scans were repeated both from the internal and the external side.

Similarly to the mock-up sample, each area scan was conducted in a 60x60 cm grid where measurement lines were obtained both in the vertical and horizontal directions with a 5 cm spacing between the lines. A grid paper with marked lines was used for marking the area, which was attached to the walls or the floor. Each measurement line consists of a number of traces (A-scans). The spacing between the traces was set to 0.5 cm, equivalent to 2 scans/cm for dense data acquisition.

5.2. Time requirements for each technology

5.2.1. AR iMMS-RGB

The data collection conducted by Microsoft HoloLens 2 and CHCNAV RS10 consisted of two processes: on-site data collection and data processing/verification. Considering the availability of the case study, the data collection was divided into two days. The afternoon of Thursday, June 12, was used to scan the upper apartment and the exterior, while the morning of Friday, June 13, was used to scan the lower apartment (and the exterior as well, to match the previous day's scan). Times are indicated in Table 10.

Table 10. Data collection time of AR iMMS-RGB measurements

Device	HoloLens 2	RS10
Day 12 (Floor 2) Scan	35 min	30 min
Day 12 (Floor 2) Process	-	65 min
Day 13 (Floor 1) Scan	30 min	12 min
Day 13 (Floor 1) Process	-	25 min

5.2.2. AHS

The most time-consuming step-in data collection with AHS is setting up the device for measurement. After defining the area to be scanned, an area sufficient for the AHS, tripod and controlling laptop needs to be cleared at about 1.5 m from the wall to be scanned. Electricity must be provided for both the AHS and the laptop, as well as cover in the case of rain/snow.

The total time used for scanning the selected areas was 2 working days. A total of 7 positions were scanned (G, C, D/E, F, H2, H1 and J2, see Table 11), with 1-6 spots (P1-6) for each area, and 1-6 scans for each spot, totalizing 76 scans (APPENDIX B). The reason for acquiring several scans for each position was to ensure the quality of the scans. Each scan required 2-3 min to be performed, which means the average time required for the actual scans was 3 hours and 10 min (assuming 2 min 30 s average time per scan). Therefore, assuming 8 hour working days, we estimate the time required for setting up the scan, as well as moving the AHS between positions, as 13 hours.

5.2.3. GPR

An initial observation of the pilot site was made to gain a better understanding of the building for scanning and to identify any limitations that had not been accounted for prior to the visit. At the same time, obstructions inside the building that could affect the scanning were removed. This took approximately 45 minutes.

The main data collection required around 6 hours for setting up the grid scans and gathering data both internally and externally. A 1-hour post-processing was carried out immediately after the data collection to verify that no issues had occurred and to check the quality of the data.

The full post-processing of the data was not conducted in Svalbard but at a later stage after the pilot site visit, and was completed within 8–10 days.

5.3. Results

5.3.1. Overview

Table 11 shows the status, size as well as the reference position of the external AHS scanning areas (SA) with respect to the building. No internal measurements were performed with the AHS.

Table 12 and Table 13 summarize the measurements for internal and external GPR SA respectively. It should be noted that some of the external SA apply to either AHS or GPR (if not applicable marked as NA), while others are common for both.

For SA in the vertical plane, A (abscissa) is the distance horizontally with positive to the right, and O (ordinate) is the distance vertically with positive upwards.

For SA in the horizontal plane, A (abscissa) is the distance in the building east-west direction, with positive towards east, and O (ordinate) is the distance in the north-south direction with positive towards north.

Table 11: AHS external scanning areas

ID	Measurement status	Size [cm]		Reference position relative (REL) to scanning area	REL [cm]	
		A	O		A	O
A	Cancelled: the plywood plate where the sample was taken has been replaced with mineral fibre plate.					
B	Cancelled due to inaccessible scanning position					
C	Scanned.	60	120 (60)	Intersection between façade plan and balcony roof/wall axis to top left of SA	0	-27
D	Scanned	50	120	Corner between façade plan and gallery roof to top right of SA	-10	-5
E	Scanned	10	120		0	-5
F	Scanned.	120	120	Corner of building and top of grill, to lower right side of SA.	0	0
G	Scanned.	120	120	Corner of building and top of grill, to lower left side of SA.	0	0
H1	Scanned.	60	60	Bottom fence and corner of building, to lower right of SA	-175	189
H2	Scanned.	60	90			0
I	Cancelled. Position Under the building. Too little headroom for equipment.					
J1	Cancelled due to inaccessibility.					
J2	Scanned. (Representative for J1).	60	60	Top of grillage/weatherboard and separation between modules to lower right of SA.	55	0
K	NA					
L	NA					

Table 12: GPR internal scanning areas

ID	Measurement status	Size [cm]		Reference position relative (REL) to scanning area	REL [cm]	
		A	O		A	O
I	Scanned	60	60	Ceiling; Wall to the left	-30	86
II	Scanned	60	60	Ceiling; Wall to the left	-56	52
III	Scanned	60	60	Ceiling; Door to the left	-98	58
IV	Scanned	60	60	Ceiling; External wall to the right	10	65
V	Scanned	60	60	Ceiling; Wall to the left	-10	65
VI	Scanned	60	60	Ceiling; Door to the left	-70	70
VII	Scanned [1]	40	40	-	-	-
VIII	Scanned	60	60	-	-	-
IX	Scanned	60	60	Floor; External wall to the left	-15	-43
X	Scanned	60	60	Ceiling; External wall to the left	-15	43
XI	Scanned	60	60	-	-	-
XII	Scanned			-	-	-
XIII	Scanned			Floor; External wall to the left	-15	-43
XIV	Scanned			Ceiling; External wall to the left	15	43
XV	Scanned			-	-	-

[1] *In addition to the 40x40 area scan, several line scans were performed*

Table 13: GPR external scanning areas

ID	Measurement status	Size [cm]		Reference position relative (REL) to scanning area	REL [cm]	
		A	O		A	O
A	NA					
B	Scanned	60	60	Roof; External wall to the right	28	60
C	Scanned	60	60	-	-	-
D	NA					
E	NA					
F	Scanned	60	60	Ground; External wall to the right	36	-130
G	Scanned	60	60	Ground; External wall to the right	25	-133
H1	NA					
H2	NA					
I	Cancelled due to difficult accessibility and equipment handling (position under the building).					
J1	Scanned	60	60	-	-	-
J2	NA					
K	Scanned	60	60	-	-	-
L	Cancelled due to inaccessibility.					

5.3.2. AR iMMS-RGB Scan

Data collection was satisfactory and proceeded without incident. The RS10 point cloud corresponding to floor 2 was manually referenced in Cloud Compare with respect to floor 1, by selecting pairs of equivalent points in the outer area, which has common overlap between both scans. Subsequently, both RS10 point clouds were merged and georeferenced to ERTS89 Zone 33N. The HoloLens 2 point clouds were also georeferenced. In post-processing, the study area was reduced to the building, eliminating points from the surrounding area, and noise points generated by the mirror effect of the windows of the upper

apartment were filtered out. The number of points is shown in Table 14 and Figure 25 and Figure 26 show images of the generated point clouds.

Table 14: Number of points

Device	HoloLens 2	RS10
Number of points	450 000	165 million

Figure 25. Point cloud generated with HoloLens 2

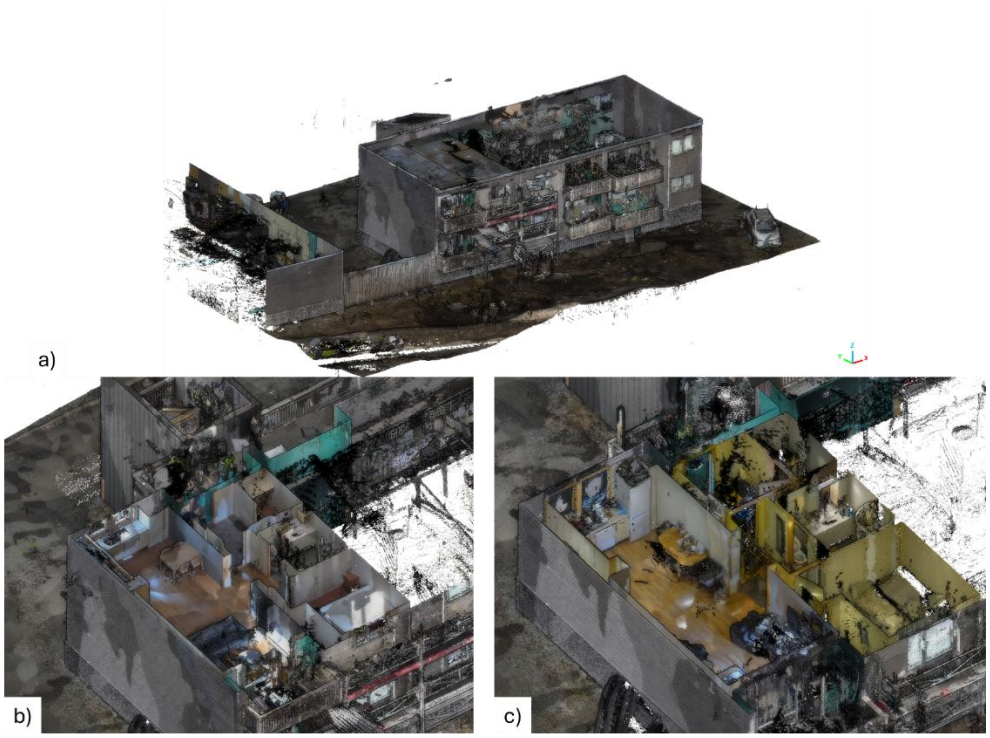

Figure 26. Point cloud generated with RS10: a) outdoor, b) apartment floor 2, c) apartment floor 1

5.3.3. AHS

Overall, the quality of the hyperspectral images was sufficient for subsequent data analysis. In locations H1, H2 and J, there were some areas of the scans that were affected by direct sunlight. However, the spectra on those scans were not compromised, and the data is still useful after processing.

Several scans presented lost pixels due to communication errors during the data acquisition. However, since multiple scans were acquired for each location, the best scan can be used for further analysis.

As mentioned in section 3.4.1, the analysis of the AHS data is dependent on the training data. In addition, as this is a completely new application for AHS, several analysis methods must be tested before any remarks can be made regarding the collected data (apart from the quality of the data, as discussed in section 3.5.2. It is not in the scope of this deliverable to discuss the various data processing and analysis methods – this will be done in deliverables 2.2 and 3.2.

5.3.4. Infrared thermography and dielectric moisture sensing

Temperature and moisture measurement didn't reveal any severe defects causing moisture traps or thermal leaks in the scanned areas (excepting area C with the damaged coating). In fact, the material was relatively dry (moisture content between 7 and 13%) due to the local climate, and the surface temperature variations were predominantly caused by direct or indirect sunlight. IRT images were re-calibrated to the emissivity 90% and background temperature 3 °C using post-processing software Fluke Connect. The lower bound of the thermographic images in areas H1 and H2 was determined by the background sky between the planks. These artefacts could be eliminated, but it was not deemed necessary as the IRT is not the main scanning method of the project. Table 15 and

Table 16 show the results of temperature and moisture measurements and example thermographs are in Figure 27 and Figure 28.

Table 15. Surface temperature obtained from the thermographic images

Location	Orientation	Max [°C]	Min [°C]	Avg [°C]	Std [°C]	Note
G	West	28,00	7,63	20,64	1,64	Direct sunlight
		31,44	13,47	25,71	2,16	Direct sunlight
D	East	2,22	-1,19	0,97	0,49	Shaded
		3,75	-0,31	1,02	0,37	Shaded
C	East	17,66	12,28	15,47	1,13	Partly shaded
		18,75	10,28	15,91	1,47	Partly shaded
H2	South	27,63	5,94	13,65	3,36	Direct sunlight, spaces between planks
		26,72	-2,06	7,53	3,64	Temporary shaded, spaces between planks
H1	South	21,97	-26,13	10,85	7,95	Direct sunlight, spaces between planks
		16,43	-2,09	9,21	3,59	Temporary shaded, spaces between planks
		18,19	-9,53	9,08	7,71	Temporary shaded, spaces between planks
		18,44	-8,00	7,60	4,25	Temporary shaded, spaces between planks
J1	South	43,13	11,63	30,63	7,86	Direct sunlight
		32,41	14,97	27,36	3,00	Direct sunlight
		31,81	14,75	26,55	3,06	Direct sunlight
		24,97	12,94	20,86	2,16	Temporary shaded
J2	South	28,91	8,78	22,93	3,11	Direct sunlight
		24,97	12,94	20,86	2,16	Temporary shaded
F	North	7,72	-0,59	2,57	0,66	Shaded
		6,91	0,88	3,48	0,51	Shaded

Table 16. Moisture content in all measuring points (left) and average value (right)

Location	Orientation	Position	Moisture
G	West	TL	11,80 %
		TR	5,20 %
		BR	7,60 %
		BL	11,10 %
D	East	TL	10,10 %
		TR	12,50 %
		BR	8,70 %
		BL	10,30 %
C	East	TL	9,60 %
		TR	11,50 %
		BR	6,90 %
		BL	8,20 %
F	North	TL	6,70 %
		TR	14,60 %
		BR	9,80 %
		BL	12,00 %
H2	South	T1	6,40 %
		T2	7,20 %
		T3	5,30 %
		T4	7,40 %
		T5	6,60 %
		B5	6,20 %
		B4	6,70 %
		B3	2,90 %
		B2	7,10 %
		B1	6,80 %
J1	South	BL	6,80 %

Location	Orientation	Moisture
C	East	9,05 %
D	East	10,40 %
F	North	10,78 %
G	West	8,93 %
H2	South	6,26 %
J1	South	6,80 %

Positions (facing towards the scanned area):
TL: top left corner
TR: top right corner
BL: bottom left corner
BR: bottom right corner
T1-T5: top of the plank number 1-5 (counted from the left)
B1-T5: bottom of the plank number 1-5 (counted from the left)

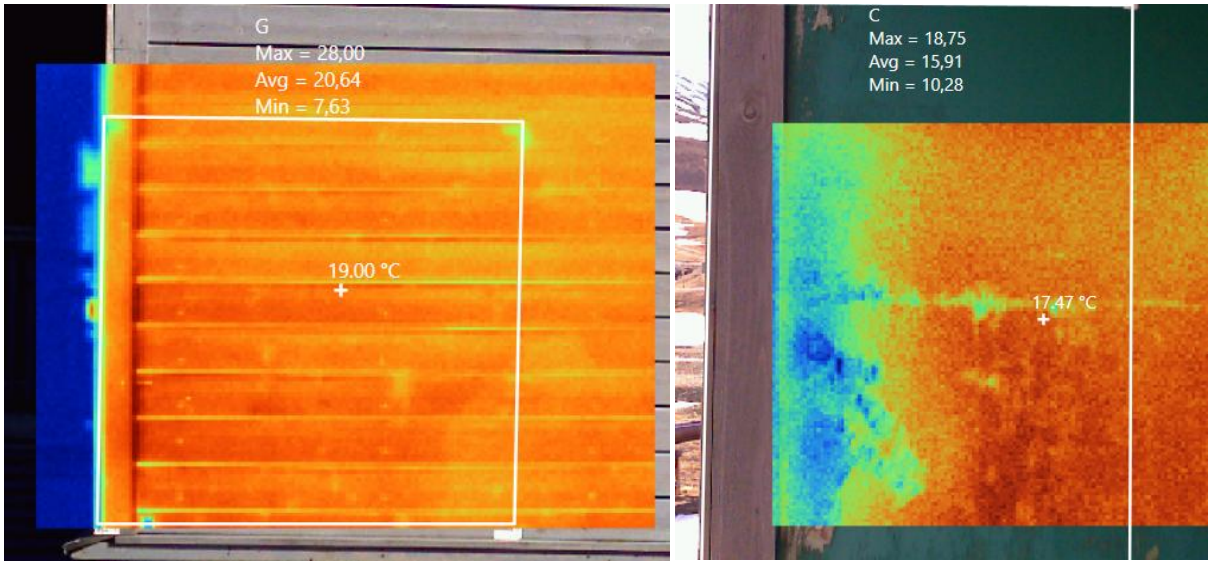

Figure 27. Example thermal images of wood cladding (left, areas F, G, J) and particle board with damaged coating (right, areas C, D)

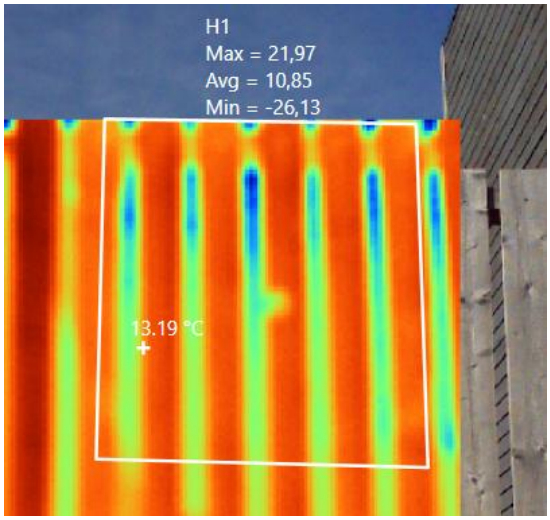

Figure 28. Example thermal image of the wooden fence (areas H1 and H2)

5.3.5. GPR

After data collection, the 24 area scan data were post-processed in the GPR Insights post-processing software using the same steps as applied in the mock-up GPR data.

Floor over foundation

Starting with the floor results, from the scans of the first floor over the foundation, the underfloor heating elements could be identified. These can be seen both in the depth-slices but also in the B-scan data as hyperbolas and were around 3 cm depth. The slice from position VIII, which shows the heating elements, is presented in Figure 29, whereas a B-scan sample from floor scan XI (middle of the living room floor) is shown in Figure 30a), from which more information can be obtained.

The floor includes also vertical wooden beams, which were also identified in the data as a strong hyperbolic response underneath the heating elements, as shown in Figure 30b).

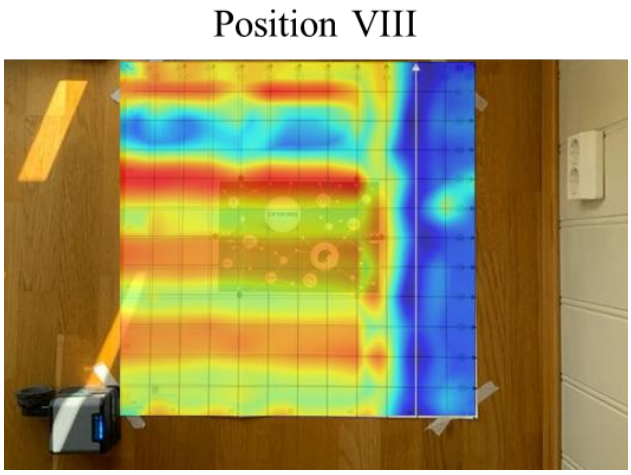

Figure 29. Depth slice from scan location VIII, where the heating elements can be observed

Floor of second floor apartment

Similar results were obtained from the floor scans over the second floor, although as observed from the GPR data, the floor structure is slightly different. The underfloor heating structure is not as clear as in the first floor, which can be observed in Figure 30a), position XV. From the B-scan data in location XII (see Figure 30b), apart from the heating elements, four interfaces between different layers can be identified. The first one is the interface between the heating elements and the insulation layer observed around 5-6 cm depth. The next two flat responses correspond to the insulation/cavity and cavity/insulation interfaces, found at 21 cm and 30 cm, respectively, which mark the cavity that exists between the two insulation layers. Deeper in the floor, the interface between the insulation and fibre board is identified.

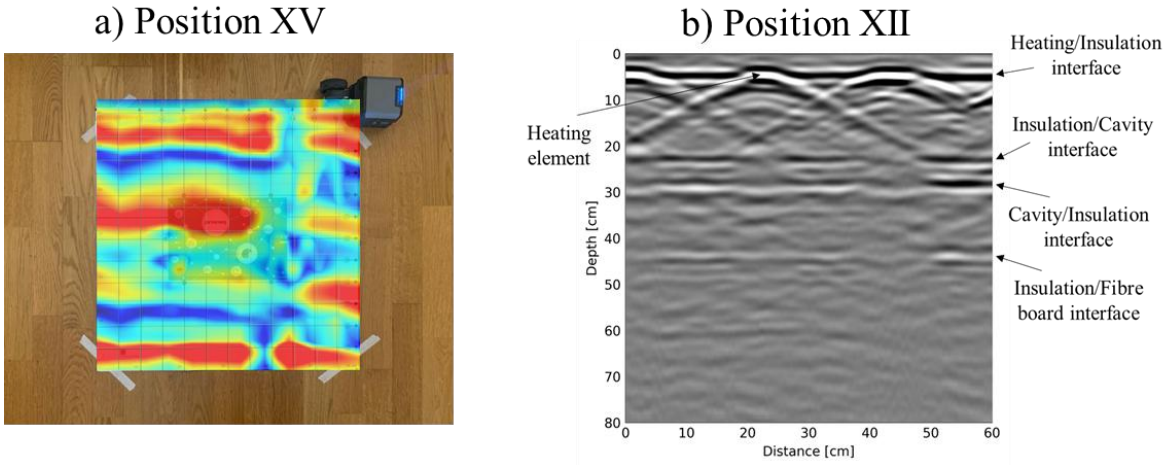

Figure 30. a) Depth slice at location XV that shows the underfloor heating and b) B-scan sample from floor scan XII in the second floor apartment.

Wall – internal scans

In all the internal scans both in the internal and external walls, the vertical and the horizontal wooden studs could be identified as these yielded quite strong responses. By internal wall, here is meant a wall between two rooms of the same apartment and an external wall, the wall of a room where there is air on the other side of the wall. Based on the slice data, the width of the studs could be estimated relatively to the other studs as thin and thicker studs were present inside the walls.

The structure of the external living room wall was common in both apartments and thus area scans in locations IX, X, XIII and XIV yielded similar results. For shortness, only location XIII

is presented here. Figure 31a) shows the location of the scan but also the depth slice at 2 cm overlaid where the vertical wooden stud can be seen. In all x-directed B-scans, another response can be seen very close to the stud, as displayed in line 7 in Figure 31b), which remains unidentified. In some of the measurements, two interfaces can be identified as shown in Figure 31b) with the first one possibly corresponding to the fibre board/insulation interface and the second one from the backwall.

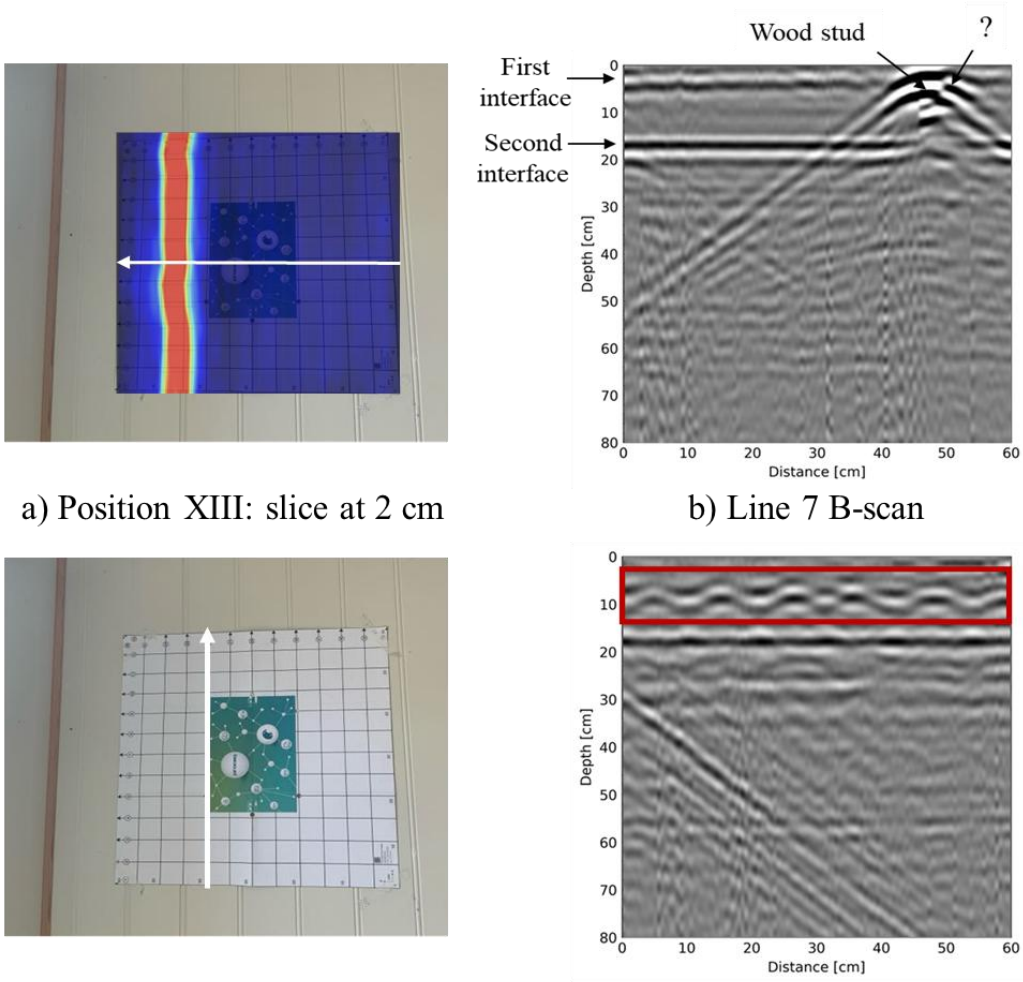

Figure 31. a) Depth slice at wall location XIII showing the vertical wooden stud identified, b) Line 7 B-scan at location XIII, c) Location of line 22 in position XIII and d) Line 22 B-scan.

Interestingly, a series of hyperbolas at the same depth of ~5 cm was found at certain locations in all walls. These are consistent and correspond to elements hidden in the wall, possibly cables or mesh and are not material inhomogeneities. An example is highlighted in Figure 31c/d) line 22, where this pattern is shown inside the insulation layer.

The internal wall between the living room and bedroom has a relatively simple structure which includes fibre board, insulation and wooden studs. The scan location on this wall can be seen in Figure 32a). The wooden stud was identified as strong hyperbolic responses at around 13 mm depth, similarly to the studs in the rest of the walls. Other flat interfaces were also observed in the GPR data, which are shown in Figure 32c) and possibly correspond to the green and red sections marked in b). These are found around 10 cm and 26 cm depth, respectively. The layers seem to be homogeneous without material variations or anomalies observed inside a layer.

The pattern of hyperbolas is also visible in the scans of this wall at ~6 cm depth, as shown by the Line 2 B-scan in Figure 32d). Since this is a repeated pattern occurring at different scan locations, it is highly likely to be structural elements inside the insulation layer.

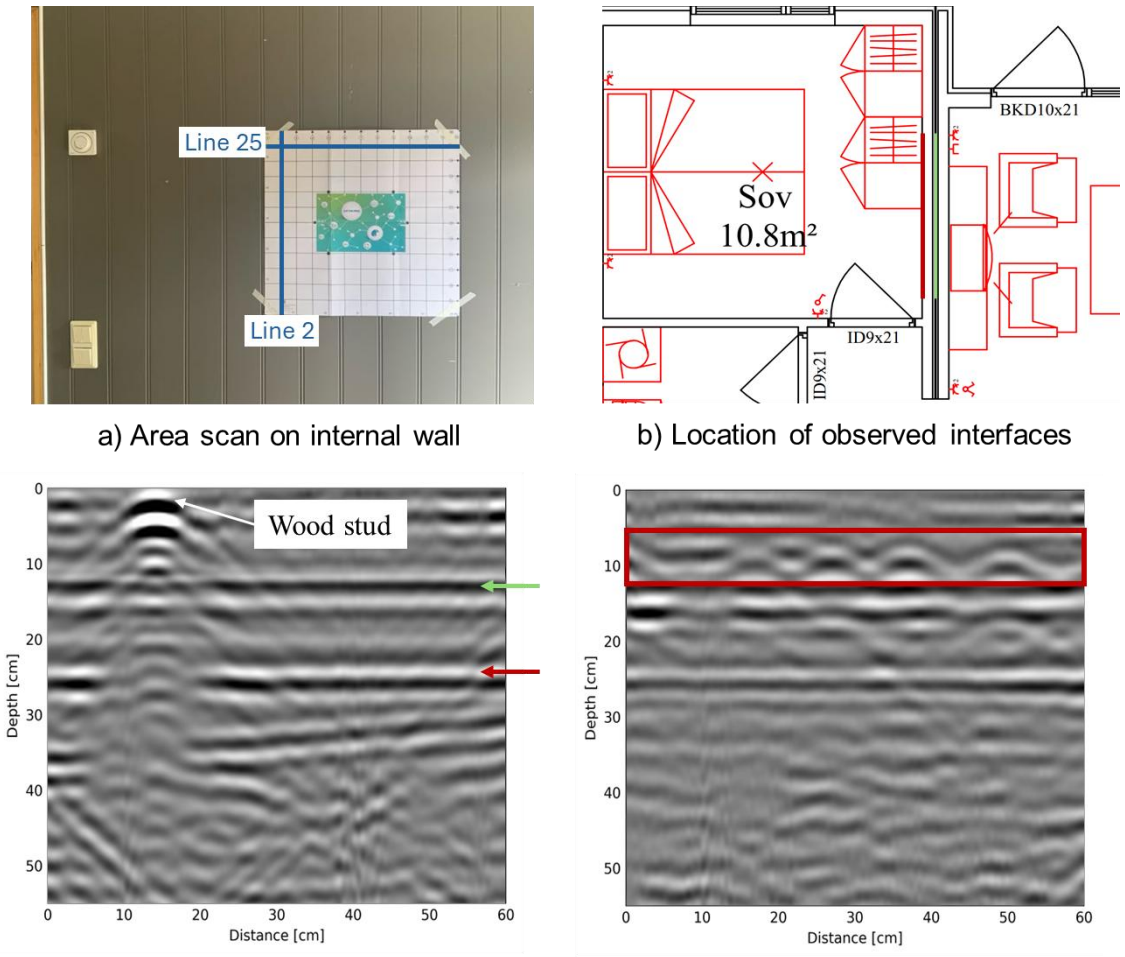

a) Area scan on internal wall

b) Location of observed interfaces

c) B-scan line 25

d) B-scan line 2

Figure 32. Results from area scan on internal wall between living room and bedroom of second floor apartment.

The bathroom wall of the second-floor apartment which is connected to the second apartment unit was also scanned (position II). The wall structure between the apartments in this case is mirrored. Two elongated targets were found in the data at ~2 cm and ~4 cm, respectively, which can be visualized in Figure 33a). By comparison, it is obvious that the one feature is thicker than the other. These could be different size studs or only one corresponding to a stud and the second response belonging to a different hidden element.

Furthermore, different interfaces between the different layers in the wall were found, namely, the fibre board/insulation, insulation/cavity and cavity/insulation interfaces as seen in Figure 33b). The latter one is from the wall mirroring in the other apartment. The interfaces are present only in some of the B-scan data

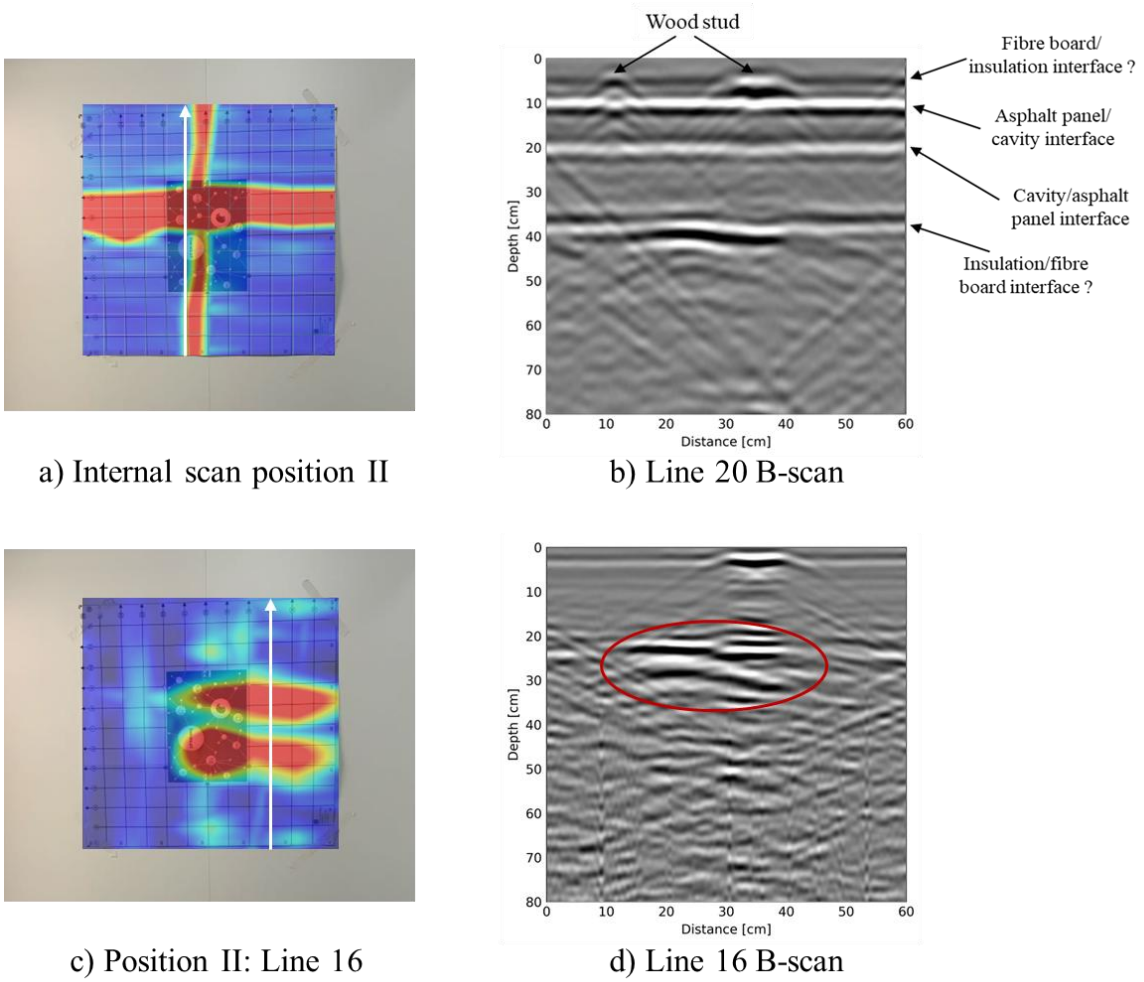

Figure 33. Internal scans on bathroom wall between the two apartments of the second floor

Deeper in the structure, around 20 cm depth, two other hidden elements are identified as presented in Figure 33c) and d). These are unlikely to be defects and could correspond to some kind of piping.

Walls – External scans

As it was expected, the external scans have significant clutter due to the cladding's irregular surface and existing gaps. This was demonstrated also in the mock-up scans presented earlier. The cladding had the highest impact on the y-directed scans, which were perpendicular to the cladding direction with an example shown in Figure 34. In addition to the gaps which are recorded on the data due to the sensitivity of the system, scanning perpendicular to the cladding did not allow for smooth movement of the system wheel and thus introducing clutter. However, by scanning parallel to the cladding direction (x-directed scans), information on certain targets was obtained. More specifically, the wooden studs, the interface between the asphalt panel/insulation and the backwall response were detected and match what was expected from the internal scans. However, unless access prevents it, it is recommended to perform internal scans instead of external in cases cladding has been installed, as the internal scans offer better data quality

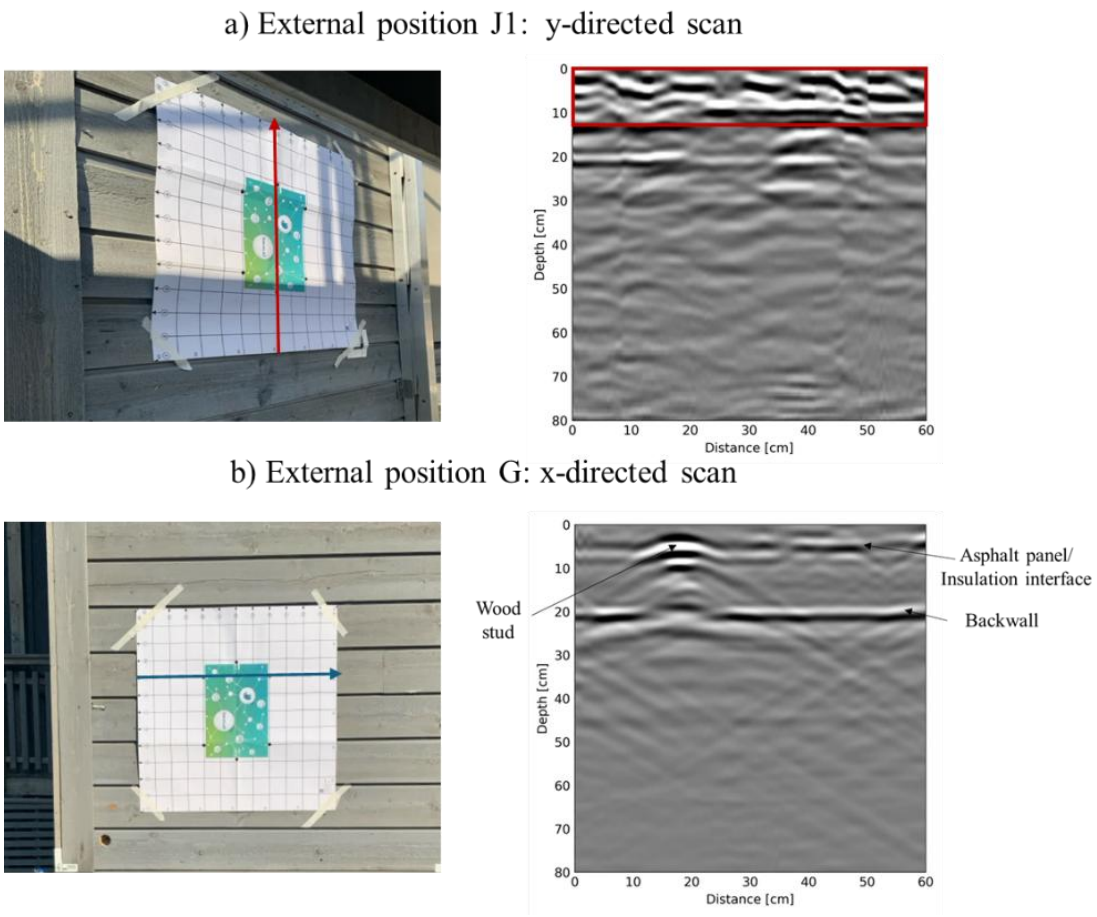

Figure 34. a) Y-directed B-scan at external position J1 illustrating the clutter caused by the cladding and b) X-directed scan at external position G showing other responses observed.

Walls external to the flat where no cladding was present were also scanned. These were a wall next to the main door (position K) and two walls in the balcony area of the second-floor apartment (positions B and C). Similar structure with studs and insulation was observed also in these areas, however there was significant clutter in the data which can be attributed to high moisture content and/or voids. Some examples can be seen in Figure 35 for position K where three B-scans are presented from lines 14, 25 and 26 which illustrate the variations observed in the data. Therefore, it is concluded from the data that this area has a high likelihood of deterioration.

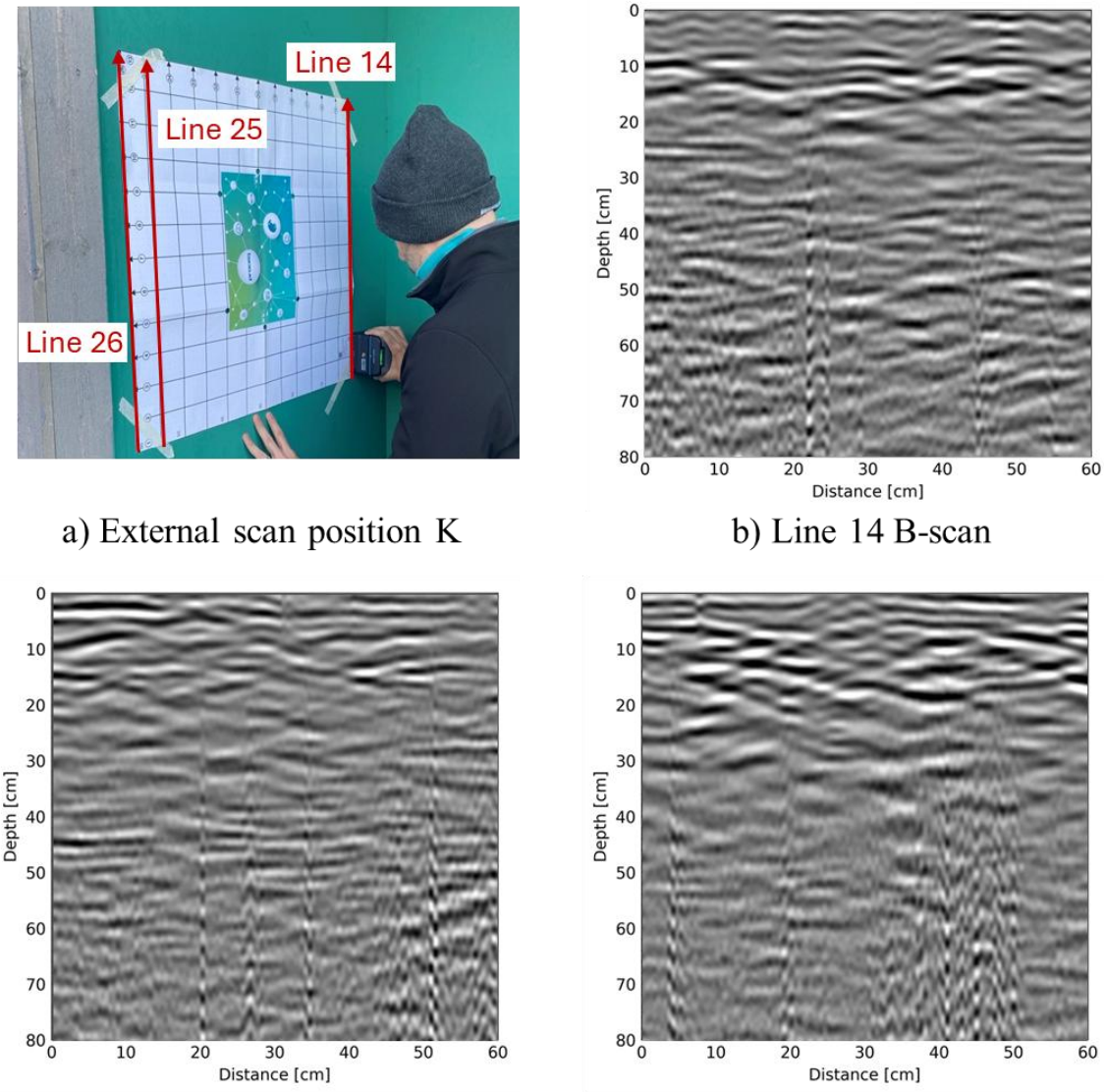

a) External scan position K

b) Line 14 B-scan

c) Line 25 B-scan

d) Line 26 B-scan

Figure 35. External wall scan position K and B-scan examples showing the variations observed in the GPR data in this wall area.

6. Conclusion

Task 10.3 has successfully established the baseline dataset for the Svalbard pilot through complementary data acquisition methods and a detailed desk-based material inventory. Active Hyperspectral Sensing (AHS) was applied to assess degradation and moisture-related risks in the timber cladding of the external walls, Ground-Penetrating Radar (GPR) enabled non-destructive mapping of subsurface construction layers and concealed elements in walls, floors and balconies, and the AR iMMS-RGB system captured the building's spatial geometry and visual condition for 3D modelling and documentation. All scanning activities proceeded according to plan, despite experienced access constraints. Some local data noise and coverage limitations were observed, particularly in GPR scans of clad external walls, mainly due to irregular surfaces and moisture effects, but these are not expected to impede subsequent interpretation and evaluation.

The collected dataset — including digital material registration in CIRDAX/CONCULAR — will serve as the technical foundation for the pilot implementation in Task 11.3. Here, the performance of the different scanning methods will be evaluated relative to traditional manual inventories with respect to effectiveness, effort reduction, and labour productivity, contributing directly to the assessment of project KPI7, which targets a 50% reduction in time for geometry and materials data acquisition and up to 90% productivity increase in hidden-component and hazardous-material identification.

Actionable recommendations are provided that will support more efficient, accurate, and circularity-focused data acquisition **in future applications** and ensure alignment with the broader objectives of the SUM4Re project**.**

ACKNOWLEDGEMENTS

Task 10.3, concerning acquisition planning, data collection, and baseline assessment for the Svalbard pilot site, has been carried out within the framework of the SUM4Re project (Creating material banks from digital urban mining). This project has received funding from the European Union's Horizon Europe research and innovation programme under grant agreement No. 101129961.

Views and opinions expressed are those of the authors only and do not necessarily reflect those of the European Union or the European Health and Digital Executive Agency (HADEA). Neither the European Union nor the granting authority can be held responsible for them.

SUM4Re

Creating materials banks
from digital urban mining

APPENDICES

Funded by the European Union. Views and opinions expressed are however those of the author(s) only and do not necessarily reflect those of the European Union. Neither the European Union nor the granting authority can be held responsible for them.

Funded by
the European Union

APPENDIX A Field records during the GPR measurements

Table 1-A. Overview of positions of performed GPR measurements (13.06.2025)

Nº	Internal/External	Storey	Room	Element type	Orientation [1)]	Distance to adjacent elements (cm)	Photos [2)]
VIII	Internal	1	Living room	Floor	-	-	1-4
IX	Internal	1	Living room	Ext. Wall	W	Floor (43); Ext. wall to the left(15)	5-6
X	Internal	1	Living room	Ext. Wall	W	Ceiling (43); Ext. wall to the left (15)	7-8
XI	Internal	1	Living room	Floor	-	-	9-10
XII	Internal	2	Living room	Floor	-	-	11-12
XIII	Internal	2	Living room	Ext. Wall	W	Floor (43); Ext. wall to the left(15)	13-14
XIV	Internal	2	Living room	Ext. Wall	W	Ceiling (43); Ext. wall to the left (15)	15-16
XV	Internal	2	Living room	Floor	-	-	17
VII	Internal	2	Kitchen	Ext. Wall	E	-	18-21
VI	Internal	2	Living room	Int. Wall	-	Ceiling (70); Door to the left (70)	22-23
V	Internal	2	Bedroom	Ext. Wall	S	Ceiling (65); Wall to the left (10)	24-25
IV	Internal	2	Bedroom	Int. Wall	-	Ceiling (65); Ext. wall to the right (10)	26-27
III	Internal	2	Bedroom	Int. Wall	-	Ceiling (58); Door to the left (98)	28-30
II	Internal	2	Bathroom	Int. Wall	-	Ceiling (52); Wall to the left (56)	31-32
I	Internal	2	Entrance hall	Int. Wall	-	Ceiling (86); Wall to the left (30)	33-36
K	External	2	-	Ext. Wall	W / E	-	37-38
F	External	1	-	Ext. Wall	N	Ground (130); Ext. Wall to the right (36)	39-40
G	External	1	-	Ext. Wall	W	Ground (133); Ext. Wall to the right (25)	41-42
J (J1)	External	1-2	-	Ext. Wall	S	-	43-46
C	External	2	-	Ext. Wall	E / W	-	47-48
B	External	2	-	Ext. Wall	W	Roof (60); Ext. wall to the right (28)	49-50

[1)] Orientation of the exposed external surface of the wall): S = South; N = North; W = West; E = East;

[2)] Available at UVigo Server_WP10_T10.3_Technical_Testing_GPR_Measurements

Table 2-A – Continuation: Overview of positions of performed GPR measurements (13.06.2025)

Nº	Comments
VIII	Located in SW corner of the building
IX	Exterior wall measurement close to floor
X	Exterior wall measurement close to ceiling
XI	Located in the middle of the flat between kitchen and living room Position was defined to measure potential differences to the results for VIII, which in contrast to XI, is located close to the facade.
XII	Nominally identical position as VIII but in second floor
XIII	Nominally identical position as IX but in second floor
XIV	Nominally identical position as X but in second floor
XV	Nominally identical position as XI but in second floor; Located in the middle of the flat between kitchen and living room; Position was defined to measure potential differences to the results for XII, which in contrast to XV, is located close to the facade.
VII	Several line-scans performed and area scan on 40 x 40 area
VI	Wall separating living room and hallway
V	Exterior wall in bedroom
IV	Interior wall separating bedroom from bedroom of adjacent flat
III	Interior wall separating bedroom from bathroom
II	Interior wall separating bathroom from bathroom in adjacent flat
I	Interior wall separating entrance hall from storage room; Wooden shelf located in the storage room behind the scanned wall (see photos 36, 37)
K	External wall with two exposure faces: W (measured) / E (backside)
F	60 x 60 area scan in approximately the middle of 120 x 120 spot marked by VTT
G	60 x 60 area scan in approximately the middle of 120 x 120 spot marked by VTT
J1	Spot located at interface between storeys 1 and 2. The 60 x 60 GPR area scan was performed in the lower right corner of the 120 x 120 square (see photo 44)
C	External wall with two exposure faces: E (measured) / W (backside) ; 60 x 60 area scan in lower half of 60 x 120 spot marked by VTT
B	Spot was not measured by VTT (no prior markings).

Funded by
the European Union

APPENDIX B AHS measurement numbering

Table 1-B: AHS measurement numbering

Position number	Spot number	Scan number (best one)
G	P1	S1
		S2
		S3
		S4
		S5
		S6
	P2	S1
		S2
		S3
		S4
		S5
	P3	S1
		S2
		S3
		S4
C	P1	**S1**
		S2
		S3
		S4
		S5
		S6
		S7
		S8
	P2	**S1**
		S2
	P3	S1
		S2
		S3
		S4
		S5
	P4	S1
		S2
		S3
	P5	**S1**
		S2
		S3
		S4
	P6	**S1**
		S2

Position number	Spot number	Scan number (best one)
D/E	P1	**S1**
		S2
	P2	**S1**
		S2
	P3	S1
		S2
	P4	S1
		S2
F	P1	**S1**
		S2
	P2	**S1**
		S2
	P3	**S1**
		S2
	P4	**S1**
		S2
H2	P1	S1
		S2
		S3
		S4
		S5
		S6
	P2	S1
		S2
		S3
H1	P1	**S1**
		S2
J2	P1	S1
		S2
		S3
		S4
	P2	S1
		S2
		S3
		S4
		S5
		S6

SUM4Re

Creating materials banks
from digital urban mining

www.sum4re.eu sum4re@uvigo.gal SUM4Re SUM4Re_EU

Funded by the European Union. Views and opinions expressed are however those of the author(s) only and do not necessarily reflect those of the European Union. Neither the European Union nor the granting authority can be held responsible for them.

Funded by the European Union